

Investigation of combustion and emissions of mixture of a wheat dust with binder pellet in a fixed-bed combustor

Saad A. El-Sayed*, Mohamed K. El-Sayed

Mechanical Power Engineering Dept., Zagazig University, Al-Sahrkia, Egypt

Corresponding Author Email: shamad53@hotmail.com

<https://doi.org/10.18280/ijht.360216>

Received: 17 October 2017

Accepted: 20 March 2018

Keywords:

wheat dust pellets, combustion and gaseous emission characteristics, internal ignition temperature, experimental correlations, ash analysis

ABSTRACT

The combustion behavior and gaseous emissions of wheat dust pellet at various operating parameters such as air temperature, pellet size, and air velocity are evaluated to achieve a better combustion performance. The results showed that as air temperature and air velocity increase as well as pellet size decreases, ignition time, char time, time to reach maximum temperature decreases and total combustion rate increases. It was concluded from the results that, a hexagonal pellet is the best shape for combustion under the investigated conditions and parameters due to its lowest ignition temperature, lowest surface temperature, shortest ignition time, and longest time required for combustion. CO₂ content reaches its maximum value at air temperature 400°C for all pellets. The maximum CO concentration occurs at the highest diameter of the pellet. The combustion efficiency ranged between 99% to 100%. The wheat dust pellet has a medium slagging tendency (slagging index=0.72) and a relatively high fouling inclination (fouling index=1.88). The activation energy of a wheat dust pellet and a binder is 102.05 and 109.62kJmol⁻¹, respectively, using TG data and kinetics model. The ignition time, the maximum combustion rate time and the burnt temperature of epoxy 1092 are lower than that of the pellet.

1. INTRODUCTION

Compared with other fossil fuels, biomass is a fuel that can produce a noticeable decrease in net carbon emissions production as well as environmental and social benefits could also be predictable [1]. Biomass is considered one of the most significant sources for producing thermal and electrical energy. Due to some disadvantages of biomass as; low density, difficulty of transportation and storage, makes the need to find fuels of higher density and hardness as pellets [2]. Biomass pellets are nowadays used in small-scale residential combustion units. Corrosion problems in combustion devices consider the main problem of using biomass pellets because of sulfur and chlorine contents in the pellet. Ignition and combustion of biomass composed of a group of complex physical and chemical processes and the ignition consider the initial main stage of combustion [3]. It was found that the rate of volatile releasing during the combustion of a large size particle depends on distribution of temperature because the pyrolysis process depends on the mechanisms of heat transfer [4]. During the devolatilization process a biomass mass loss occurs rapidly, this lets it ignite faster at low temperature compared to the coal. The temperature of solid and gas phases is not the same during the combustion of solid fuel. So, there is a temperature deviation that leads to the transfer of heat between the two phases [5-6]. When pellets are heated, temperature gradients are set up in it. As heat propagates into the pellet, moisture is evaporated and when the pellet surface becomes enough hot, a thermal decomposition process takes place which known as pyrolysis. The gaseous volatile released during the thermal decomposition reacts with the oxidant leaving a residual char. As the surface of the pellet becomes

hotter, more volatiles released from inside the pellet leading to an extra devolatilization [3]. The char layer that is left behind undergoes heterogeneous combustion releasing heat (char combustion). Gaseous emissions from biomass combustion are almost depends upon the properties of biomass and the operating conditions in the combustion devices. Reducing the gas emissions become now the main target in the recent development of the biomass heating equipment [7-8]. The combustion characteristics and environmental performance of pelletized hardwood of aspen such as emissions and slagging under different conditions has been studied by ref. [9]. A single wooden sphere pyrolysis and ignition exposed to a stream of hot air under different operating conditions has been investigated in ref. [10]. Impregnation of olive mill wastewater on dry biomasses and studying the impact on chemical properties and combustion performances has been investigated in ref. [11].

Different work in a fixed bed combustor necessitate its steady-state operation, in order that models can be handled mathematically and may be verified experimentally [12]. Two fundamental scale parameters which used to analyze or compare the behavior of combustion of the different biomass fuels in the combustors are the devolatilization and char times. A kinetics data for biomass are usually determined by TG/DTG which aid in pyrolysis behavior inside the real combustors. Thermal decomposition and kinetic parameters under inert or oxidant atmosphere are investigated and determined for some biomass fuels in refs. [13-14]. Physico-chemical properties and thermal degradation characteristics of agro pellets from olive mill by-products/sawdust blends has been investigated in ref. [15]. Thermal analysis and devolatilization kinetics of the cotton stalk, sugar cane bagasse

and shea meal under nitrogen and air atmospheres has been studied in ref. [16].

The main gaseous emission characteristics of biomass fuel combustion such as CH₄, CO₂, CO, H₂O, NO_x and other hydrocarbons investigated both qualitatively and quantitatively in ref. [17]. NO_x component is negligible compared to other gases in the fixed bed combustor as shown in ref. [18]. A severe decrease in O₂ and a rise in CO₂ and CO at the start of the combustion process is reported in ref. [19]. On the other hand, an intense decrease in CO₂ and CO during char combustion is noticed in ref. [20].

Slag, deposit formation, and emissions of fine particle are the main problems of producing ash of biomass combustion, which decrease the combustor performance is studied in ref. [21]. The mineral species which are commonly found in biomass will cause both erosion and abrasion problems [22]. The control of emission gas temperature and some additives can be used to reduce or prevent corrosion as reported in ref. [23].

The object of this work is to study the combustion and emissions of wheat dust pellets with a chemical binder (Epoxy1092) under different operating conditions such as pellet size [Cylindrical pellet (of different dimensions) 42 mm long and 18, 10 mm in diameter, respectively, and hexagonal pellet (new shape) with side length = 6 mm and 42 mm long (D3)], starting air temperature from [400-180°C] and primary air flow velocity from [4.2 to 3.2 m s⁻¹] in a fixed bed combustor. The first part of this study focuses on using the TGA to study the combustion parameters and the apparent kinetics of wheat dust pellet and chemical binder (Epoxy1092) because the TGA results were very important to be determined before the beginning of actual combustion in the FBC. The second part of this article is studying the combustion behavior of the wheat dust pellet as the surface and central temperatures of the pellet, the time dependent mass loss rates of pellet, emission characteristics of the pellet as well as a simple combustion ash analysis are recorded to achieve maximum temperatures at the pellet surface, the maximum char combustion time and total fuel combustion time. Correlations between the input parameters and the combustion parameters using the data fit methods will be presented.

2. EXPERIMENTS

2.1 Pellet Preparation

Wheat dust samples were collected from local farms in Egypt at Al-Sahrkia Governate. The wheat was harvested in May 2016 and the wheat dust was sun dried for 3 days to reduce the moisture. The small, elongated pieces of wheat dust samples were entered the milling machine which has 3 hammer knives and electric power 1.84 kW, to produce the fine powders. The particle mean diameter and its standard deviation are 0.467mm and 0.277mm, respectively from sieving and statistical analysis. The wheat dust powder is mixed with 40% binder (Epoxy 1092). Epoxy consists of resin Araldite PY 1092-1 (100 part by weight) and hardener HY 1092 (50 part by weight). The viscosity of the two parts is 0.4 Pa.s at 25°C, density (g/cm³) at 25°C is 1.15 and 1.0 for the two parts, respectively. The reasons of addition binder [epoxy 1092] during production of pellets: excellent mechanical properties as this binder increases the durability and hardness of pellet which make pellet easy for handling and transporting,

low cost, excellent chemical resistance, very good processing properties and low viscosity of the system which facilitates its manual application when we mix the binder and wheat dust powder. Then, the mixture of [wheat dust and binder] is inserted into a mold and compressed by a hydraulic pressing unit at pressure 15 bar and kept in 60 sec. This hydraulic pressing unit consists of a hydraulic pump and a piston connected to the upper moving crosshead of this unit. Cylindrical molds (of different dimensions) 42 mm long and 18, 10 mm in diameter (D1, D2) respectively, and hexagonal die with side length = 6 mm and 42 mm long (D3) were used in this study. The dies were slip fit into a base made of stainless steel with a bore matching the die outer diameter. This base supported the complete structure and also allowed the piston to move upright down without any lateral movement during the process of compression. The weights of wheat dust pellets are (15.3mg±0.65%) for cylindrical pellet with diameter 18mm and length 42mm, (10mg±1.00%) for cylindrical pellet with diameter 10mm and length 42mm and (7.8mg±1.28%) for hexagonal pellet with diameter 18mm and long 42mm. Figure 1-a illustrated the detailed morphological information of acquired pellets by using a scanning electron microscope (SEM Model Quanta 250 FEG) and figure 1-b illustrated the micrographical image of the outer surface of the pellets. It can be seen in figures (1-a and 1-b) that due to the compression process, flat-shaped particles of wheat dust and binder particles may interlock each other, producing interlocking bonds.

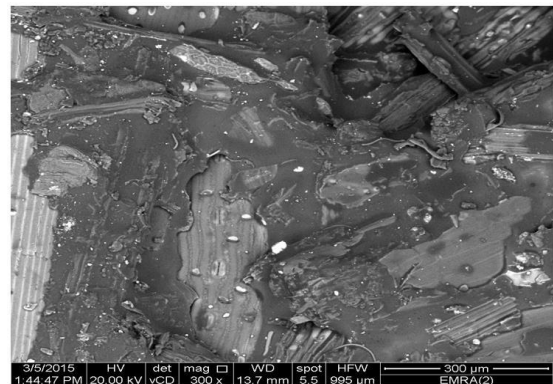


Figure 1a. Scanning electron image of the outer surface of wheat dust pellets



Figure 1b. Micrograph image of the outer surface of wheat dust pellets

2.2 Proximate and ultimate analyses of fuel

Proximate analysis measurements were done by the TGA

and the main elements of the biomass such as moisture content, volatile matter, ash and fixed carbon are given in table 1. The ultimate analysis of the wheat dust pellet was performed using a CHNOS elemental analyzer (Model Vario EL III) to measure carbon, hydrogen, nitrogen, sulfur, and oxygen content was calculated by a difference as shown in table 1. The HHV (higher heating value) of the materials was measured using a Barr oxygen bomb calorimeter, (Model 1341EE Plain Oxygen Bomb Calorimeter).

Table 1. The proximate analysis, ultimate analysis and heating value of raw wheat dust, wheat dust pellet and binder

Analysis	Wheat dust	Epoxy 1092	Wheat dust pellet
Proximate analysis, %			
Moisture	2.9	0.0	3.9
Volatile matter	72.1	87.41	76.2
Fixed carbon	8.3	8.31	10.8
Ash	16.7	4.28	9.1
Ultimate analysis, %			
Carbon	39.21	70.56	65.5
Hydrogen	6.44	7.80	5.04
Oxygen	52.83	17.18	27.1
Nitrogen	1.11	4.18	1.77
Sulfur	0.41	0.28	0.59
Heating value (kJ kg ⁻¹)	14610.35	34000	25350.4

2.3 TGA experiments

Thermogravimetric analyses (TGA) experiments were performed by a thermal analyzer (Shimadzu TGA-50). All experiments were conducted under atmospheric pressure, the temperature range is from ambient to 1000°C and a heating rate of (30) Kmin⁻¹ under a nitrogen flow rate of 30 ml min⁻¹ and the gas supply was controlled by calibrated volume flow meters. Limited by the size of the sample pan, the pellet was broken into small parts using a razor blade manually, a small mass approximately 2.15mg for raw wheat dust, 13.56 mg for wheat dust pellet and 6.70 mg for epoxy 1092 were used for TG tests. The simultaneous mass loss and temperature data were obtained. These data were used to determine the kinetic parameters as activation energy, frequency factor, and reaction order as we will see later.

2.4 Combustion characteristic parameters

A series of important combustion parameters and their indices for wheat dust pellet and epoxy 1092, were defined from TG/DTG profiles and then calculated. These parameters include ignition temperature (T_i); which defined as the temperature at which a sudden decrease in mass loss on the DTG curve occurred. The ignition index (D_i); defines how fast the fuel is ignited. Also, other parameters as maximum combustion rate (V_{max}) (i.e. the maximum of the mass-loss rate during the combustion process) and its corresponding temperature (T_{max}), average combustion rate (V_{mean}), burnout temperature (T_f); which defined as the temperature at which the mass-loss rate is smaller than -0.01mg min⁻¹ and its corresponding burnout index (D_f), and the combustion characteristic index (S) [24-25]. The ignition index (D_i) is determined by the following equation:

$$D_i = \frac{V_{max}}{t_p t_i} \quad (1)$$

where: t_p and t_i are the corresponding time of the maximum combustion rate and ignition temperature, respectively. The mean combustion rate (V_{mean}) represents the mean mass loss rate during the entire combustion process, and it is determined by the following equation:

$$V_{mean} = \frac{m_1 - m_2}{t} \quad (2)$$

where: (m₁) is the mass of the sample at ignition temperature (T_i), (m₂) is the mass of the sample at a burnout temperature (T_f), and (t) is the time zone from T_i to T_f. Also, the burnout index is used to evaluate the burnout performance, which can be described as follows [26]:

$$D_f = \frac{V_{max}}{\Delta t_{1/2} t_p t_f} \quad (3)$$

where: Δt_{1/2} is the time zone of $\frac{(dw/dt)}{V_{max}} = 1/2$ and t_f is the burnout time. The combustion characteristic index (S) can be determined by the following equation [27-28]:

$$S = \frac{V_{max} \times V_{mean}}{T_i^2 \times T_f} \quad (4)$$

2.5 Kinetic parameters estimation

Generally, the thermal decomposition of biomass is expressed by the following equation:

$$\frac{d\alpha}{dt} = kf(\alpha) \quad (5)$$

where f(α): A function, the type of which depends on the reaction mechanism. α: The degree of conversion and is normalized form of weight loss data of decomposed sample and is defined by the expression:

$$\alpha = \frac{m_i - m_t}{m_i - m_f} \quad (6)$$

where m_i: The initial mass of the sample, mg. m_f: The final mass of the sample, mg. m_t: The sample mass at temperature T, mg. k, is the temperature dependent rate constant, usually described by Arrhenius equation as:

$$k = Ae^{-\left(\frac{E_a}{RT}\right)} \quad (7)$$

where A: The pre-exponential or frequency factor, min⁻¹, E_a: The activation energy of the decomposition reaction, (kJ mol⁻¹), R: The universal gas constant (8.314 kJ mol⁻¹ K⁻¹), T: The absolute temperature, K. Inserting an Eq. (7) in Eq. (5) gives;

$$\frac{d\alpha}{dt} = Ae^{-\left(\frac{E_a}{RT}\right)} f(\alpha) \quad (8)$$

According to the uniform kinetics of the reaction, f(α) can be defined as

$$f(\alpha) = (1 - \alpha)^n \quad (9)$$

where n: The order of reaction. Substituting an expression (9) into the Eq. (8) gives the expression of reaction rate in the form

$$\frac{d\alpha}{dt} = A e^{-\frac{E_a}{RT}} (1 - \alpha)^n \quad (10)$$

In non-isothermal TGA experiments, the heating rate vary as a function of time

$$\frac{d\alpha}{dT} = \frac{d\alpha}{dt} \times \frac{dt}{dT} \quad (11)$$

For non-isothermal measurements with a linear heating rate, $\beta = \frac{dT}{dt}$, Eq. (11) can be rewritten as

$$\frac{d\alpha}{dT} = \frac{d\alpha}{dt} \times \frac{1}{\beta} \quad (12)$$

Hence Eq. (12) can be rewritten in the final form as

$$\frac{d\alpha}{dT} = \frac{A}{\beta} e^{-\frac{E_a}{RT}} (1 - \alpha)^n \quad (13)$$

$\frac{d\alpha}{dt}$ can be obtained by taking the first derivative of Eq. (6) as:

$$\frac{d\alpha}{dt} = \frac{-1}{m_i - m_f} \times \frac{dm_t}{dt} \quad (14)$$

So, the Eq. (14) expresses the fraction of material consumed in the given time. In this work the activation energy was obtained from the non-isothermal TGA. Several methods can be used to estimate kinetic parameters and one of them is Coats–Redfern method [29]. The following equations are used for this analysis:

$$\text{Ln} \left[\frac{1 - (1 - \alpha)^{1-n}}{T^2(1-n)^n} \right] = \text{Ln} \left[\frac{AR}{\beta E_a} \left(1 - \frac{2RT}{E_a} \right) - \frac{E_a}{RT} \right] \quad (\text{for } n \neq 1) \quad (15)$$

Since the term $\frac{2RT}{E} \ll 1$, so Eq. (15) becomes:

$$\text{Ln} \left[\frac{1 - (1 - \alpha)^{1-n}}{T^2(1-n)^n} \right] = \text{Ln} \left[\frac{AR}{\beta E_a} \right] - \frac{E_a}{RT} \quad (\text{for } n \neq 1) \quad (16)$$

The same notations Y and X can be used also in Eqs. (16) as

$$Y = \text{Ln} \left[\frac{1 - (1 - \alpha)^{1-n}}{T^2(1-n)^n} \right] \text{ versus } X = \frac{1}{T} \quad (\text{for } n \neq 1) \quad (17)$$

Plots of Y versus X are obtained at various values of n, to determine the correct reaction order. All the data obtained at different values of (n) were fitted and the best-fit regression line that has the highest value of the correlation coefficient (R^2) was determined. The slope of the fitted straight line of the plot represents $\frac{-E_a}{R}$, which can be used to evaluate the activation energy. The frequency factor can be determined from the intercept of the line with the vertical axis.

2.6 Ignition and combustion experiments in the fixed bed combustor

The experimental setup schematic diagram used in this work is illustrated in figure 2. The setup consists of : (a) a series of three modular components, these components were made up of a thick steel sheet and connected through flanges and each component contains two parallel heaters of 1.0 kW to adjust air temperature entering the fixed bed combustor and

switched according to the temperature required, (b) a combustion chamber (90 cm long and 30 cm inner diameter) that was placed vertically, (c) stationary calibrated thermocouples (type K) were fixed at pellet surface, pellet center, and near the top and bottom surfaces of the pellet which they used to measure gas temperature and these thermocouples were connected to a multichannel digital data logging thermometer [TM-747DU of accuracy $\pm 0.1\% + 0.7^\circ\text{C}$] that was connected to a computer, (d) a balance has a readability of 0.1g and can measure up to 2000 g made by BROTHER is placed on a well-insulated stable board below the combustor. It is completely separated from the combustor so that its movements and vibrations do not interfere with balance measurements, (e) a gas analyzer IMR 3000P is used to measure the temperature and concentrations of gaseous emissions as O_2 , CO and CO_2 , with measurement errors of: O_2 , ± 0.1 vol. %; CO, ± 0.0001 vol. %; and CO_2 , ± 0.1 vol. %, (g) an air distributed plate that constructed from perforated steel plate in a definite geometric pattern and it is positioned at the entrance of the combustor test section. The distributed plate of 32mm outer diameter had 52 holes (each about 3mm in diameter) and it is used to provide a uniform air distribution inside the combustor. The pellet is located in the center of the combustor test section to be far away the velocity boundary layer. The combustor outer wall was insulated with ceramic-fiber material of 100mm thick and covered from outside by 1-mm thick galvanized steel sheet. A time interval between pellet entering the furnace until it reached their designated position was approximately 0.4–0.8 s and the response time of the thermocouple is 0.5 s. A blower supplies air to the combustor and the velocity and pressure of the delivering air were monitored by air PVM100 micromanometer with accuracy $\pm 1\%$ of reading ± 1 digit and pressure resolution 1 pa. The flowing air is preheated by the electric heaters, then passes to the bottom surface of the pellet as a forced flow to enhance mass and heat transfer between the solid and the gaseous phases. The pellet was inserted in the combustor test section when the air and wall temperature became almost steady after 2hr for a high air temperature to 1hr for a low air temperature. The measuring instruments were used to measure and record: the weight loss, the temperature changes on the surface, the temperature changes in the pellet center, and emission gases concentrations. The essential operating parameters in these experiments were selected according to the facilities of the experimental setup as follows: temperature ranges from 180–400°C, air flow velocity ranges from 3.2–4.2 ms^{-1} , and fuel sample diameter ranges from 6 to 18 mm. The thermal conductivity k_s and the specific heat C_p of wheat dust [30] are 0.13 $\text{Wm}^{-1}\text{K}^{-1}$ and 1.63 $\text{kJ kg}^{-1} \text{K}^{-1}$ at 300K. The thermal conductivity of epoxy 1092 is generally low and equals 0.2 $\text{Wm}^{-1}\text{K}^{-1}$ and the specific heat $C_p = 1.2 \text{kJ kg}^{-1} \text{K}^{-1}$. Tests conditions are listed in Table 2. The Reynolds number (Re_d) is based on the cylinder's diameter, and the mean local velocity, V_a , of the air around the pellet. The heat transfer coefficient was determined according to the [Ranz–Marshall [31] correlation:

$$h = (k_a/d_o) (2 + 0.54Re_d^{0.5}) \quad (18)$$

where: h ($\text{Wm}^{-2}\text{K}^{-1}$) is the heat transfer coefficient, k_a ($\text{Wm}^{-1}\text{K}^{-1}$) is the thermal conductivity of air, d_o is the diameter of the pellet and Re_d is the Reynolds number based on the pellet diameter.

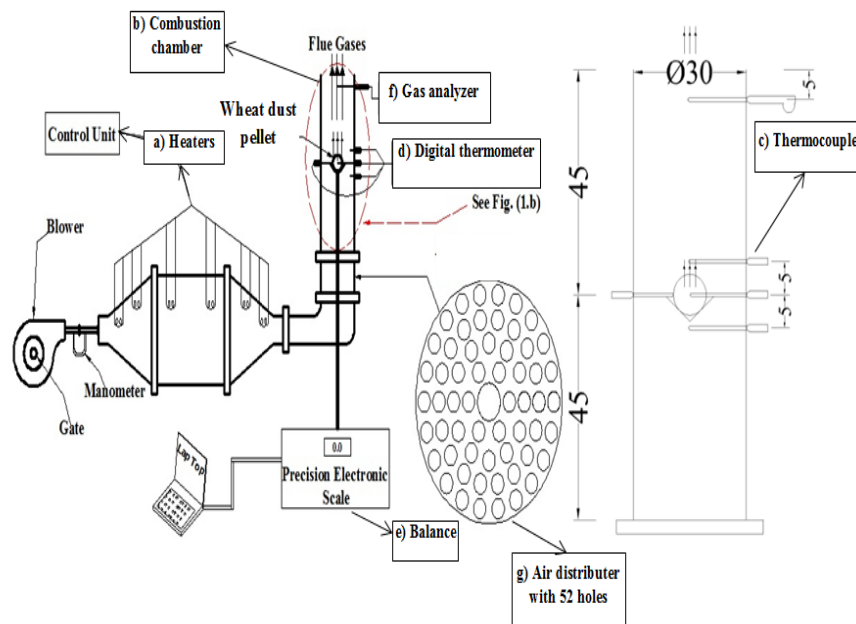
Table 2. Tests conditions

T_a K	Cylindrical pellet $d_o=18\text{mm}$			Cylindrical pellet $d_o=10\text{mm}$			Hexagonal pellet $S=6\text{mm}$		
	Re_d	h	$h(T_a-T_o)$	Re_d	h	$h(T_a-T_o)$	h	$h(T_a-T_o)$	
		$\text{Wm}^{-2}\text{K}^{-1}$	kWm^{-2}		$\text{Wm}^{-2}\text{K}^{-1}$	kWm^{-2}	$\text{Wm}^{-2}\text{K}^{-1}$	kWm^{-2}	
673	1184.22	58.32	21.75	657.9	80.84	30.15	683.56	79.12	29.5
593	1462.47	57.88	16.96	812.48	59.23	23.44	884.17	78.31	22.95
533	1748.99	58.47	13.62	971.66	80.62	18.78	1009.56	78.96	18.39
453	2306.71	58.04	8.88	1281.53	79.77	12.21	1331.46	78.12	11.95

where T_a = air stream temperature, K.

Since the bottom surface area of the pellet subjected to the air flowing is considered small (no more than about 14 % of the initial surface area) during the experiments, the influence of changes in the flow momentum on the mass loss measurements is neglected. In the first stage of the pellet conversion, heat is transferred from the hot air to the surface of the pellet by convection and radiation. The heating up process continues until the pellet surface temperature reaches a certain value beyond which, the biomass starts to decompose into volatiles matters (e.g., H_2O , CO , CO_2 , CH_4) and char

residue. Once gaseous species are formed, they move through the biomass solid bores to the pellet surface where they react with the hot air. On the other hand, this flow of volatiles will resist the oxygen diffusion to the pellet surface to react with the formed char during the pyrolysis process. So, the char combustion may or may not take place at the same time with devolatilization and homogeneous reactions near of the pellet. This ignition behavior can be defined as a “multistage” process, since it involves a primary heterogeneous ignition of pellet with a subsequent homogeneous ignition and combustion of volatiles.



3. DISCUSSION OF THE RESULTS

3.1 TGA analysis

TGA experiments were carried out to understand the thermochemical characteristics of the wheat dust pellet and epoxy 1092. Figure 3 shows TG/DTG profiles for both wheat dust pellet and epoxy1092. Drying is the first step where a biomass sample is exposed to high temperatures. During this stage, the temperature of the biomass increases, and once the layer of moisture in the sample reach the boiling temperature (100°C), all energy is used to evaporate water until the sample gets dry. The time required for heating is linearly dependent on the moisture content and quadratically on the sample size [32]. From the present results the water content for wheat dust pellet may be estimated to be about 4 wt. % owing to the observed mass loss below 200°C . For the wet sample, the evaporation required more energy as moisture is concentrated in the

material cell walls. This energy was taken from the inert gas, which in turn delayed the time at which volatiles released. These results run with that published by [33]. As the heating process proceeds where the temperature is around 260 to 300°C , chemical decomposition of biomass occurs [34] and this is called devolatilization stage. During the devolatilization stage, the organic structure of biomass decomposes. Both homogeneous and heterogeneous reactions occur during devolatilization stage. After volatiles release from the pellet, it will ignite homogeneously with atmospheric air. At some point, the surface temperature reaches the surrounding gas temperature and passes. Mass loss during devolatilization stage occurs at a high rate and the rate soon reaches a maximum, followed by a period of decreasing values. The sample loses almost 80% of its mass (depending on its volatile content) during this stage. The estimated contents of volatile matter are 76.2 wt. % for wheat dust pellet and 87.41 wt. % for epoxy 1092 at temperature ranged between 200 and 400°C .

Volatile matters have a high reactivity, and it is nearly accompanied with ignition temperature. Most of the mass loss in the second region is due to the thermal breaking of weak bonds in the structure of the main compositions of the biomass. The last stage is char burning, which commences at around 400 to 600°C [34] when there are no volatile or moisture left in the sample. During this stage, char (a carbon rich solid residue), converts slowly to ash and carbon dioxide. Char burning occurs at much lower rates compared to previous stages of combustion. Char burning rate is mainly controlled by oxygen diffusion from the gas to the char surface, at which it reacts with char to form ash and carbon dioxide. The fixed carbon can be estimated to be about 10.8 wt. % for pellets and 8.31wt. % for epoxy1092 at temperature ranged between 400 and 600°C. The content of the ash, where the reaction process is almost ended, is approximated about 9.1wt. % for wheat dust pellets and 4.28wt. % for epoxy 1092. The TGA results were very important to be determined before the beginning of actual combustion in the fixed bed combustor. Because the startup temperature at which the air introduced to the combustor was determined based on the values of temperatures at which the devolatilization and hemicelluloses decomposition occurred for pellet. The startup air temperature in real combustors was taken above the temperature at which the moisture releases [35-36]. The minimum value of startup temperature was taken above 200°C to help the volatile matter to release easily from material and increase the reaction rate of the char formed after volatile release, which in turn increases the hemicellulose decomposition rate. The Ignition temperature of wheat dust pellet and the binder is 138°C, 207.9°C, respectively. The lower the ignition temperature is, the better combustion reactivity of the pellet. The peak temperature on the DTG curve is equal 398.1°C, 355.97°C for wheat dust pellet and epoxy1092, respectively. The peak temperature is a measure of fuel reactivity (at the maximum rate of weight loss $(dm/dt)_{max}$) due to volatilization accompanied by the formation of carbonaceous residue. Burnout temperature is equal 705°C, 574.14°C for wheat dust pellet and epoxy1092, respectively. High burnout temperature shows that pellet burning will be more difficult and needs longer residence time and a higher temperature to reach complete combustion. The ignition time of wheat dust pellet and epoxy 1092 is 4 and 2 min, respectively, the time to reach a maximum combustion rate of wheat dust pellet and epoxy 1092 is 12.73 and 6.01 min, respectively, but the burnout time of wheat dust pellet and epoxy 1092 is 23 and 15 min respectively. The ignition index of wheat dust pellet and epoxy1092 is 80.23×10^{-3} and $220.28 \times 10^{-3} \text{ mgmin}^{-1}$ respectively, the burnt characteristics of wheat dust pellet and epoxy1092 is 9.56×10^{-4} and $45.53 \times 10^{-4} \text{ mg min}^{-4}$. The larger the ignition index and the burnout index are, the higher the combustion activity of fuel. The calculated combustion characteristic parameters are listed in table 3. The integral method as explained before is used to determine (n), (E_a), and (A) of the tested material. Kinetics of biomass are classified

into devolatilization and combustion stages as shown in figure 4, where $[Y = \text{Ln} [\frac{1-(1-\alpha)^{1-n}}{T^2(1-n)}]]$ and $X = \frac{1}{T}$. The (E_a) and (A) values can be determined from the slope and intercept of the best fit straight line whose the highest correlation coefficient R², respectively. The plots showed good linearity of the data with high value of the regression coefficient (R²) which is mainly above 90%. Table 4 presents the kinetic parameters values of both wheat dust pellet and epoxy 1092. Generally, activation energy and pre-exponential factor values of wheat dust pellet are lower compared to those values of epoxy 1092. This deviation in activation energy could be caused by the influence of heat transfer at high temperatures, these kinetic parameters may help the development of the conversion of these abundant biomasses into energy. In fact, the obtained values from the kinetic study are useful for the configuration and the designing of the suitable reactor.

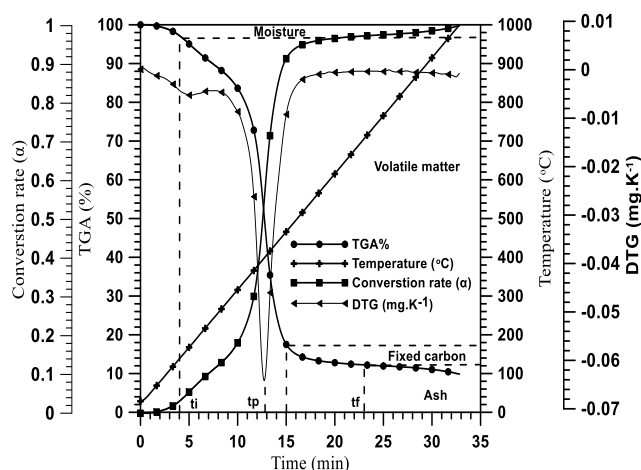


Figure 3a. TGA and DTG for wheat straw pellet

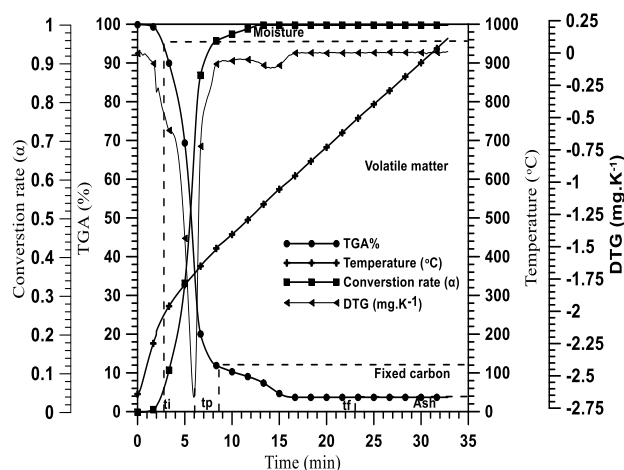


Figure 3b. TGA and DTG for epoxy 1092

Table 3. Combustion characteristic parameters of wheat dust pellet and epoxy 1092

Samples	T _i °C	t _i min	T _{max} °C	t _p min	V _{max} mg min ⁻¹	t _f min	T _f °C	V _{mean} mgmin ⁻¹	D _i ×10 ⁻³ mgmin ⁻³	D _f ×10 ⁻⁴ mgmin ⁻⁴	S×10 ⁻⁹ mg ² min ⁻² .°C ⁻³
Wheat dust pelle	138	4	398.1	12.73	3.85	23	705	0.37	80.23	9.56	106.58
Epoxy	180	2	355.97	6.01	2.65	15	571.14	0.19	220.28	45.53	26.58

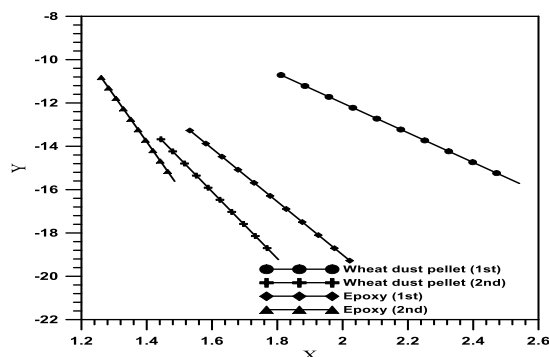


Figure 4. Y–X curves for the first and second zones of wheat dust pellet and epoxy 1092 for the integral method

Table 4. Kinetic parameters of wheat dust pellet and epoxy 1092

Fuel type	Stage no	Reaction order, n	Activation energy, E(kJmol ⁻¹)	Frequency factor, A (min ⁻¹)	R ²
Wheat dust pellet	Stage 1 [120→280] °C	1.6	52.86	4.09x10 ⁻³	0.94
	Stage 2 [280.6→420.3] °C	1.5	151.25	1.223x10 ⁻³	0.95
Epoxy 1092	Stage 1 [120.1→400] °C	1.3	99.06	8.08x10 ⁻⁴	0.95
	Stage 2 [400→520] °C	1.4	120.19	9.802x10 ⁻⁴	0.95

3.2 Combustion behavior of wheat dust pellet

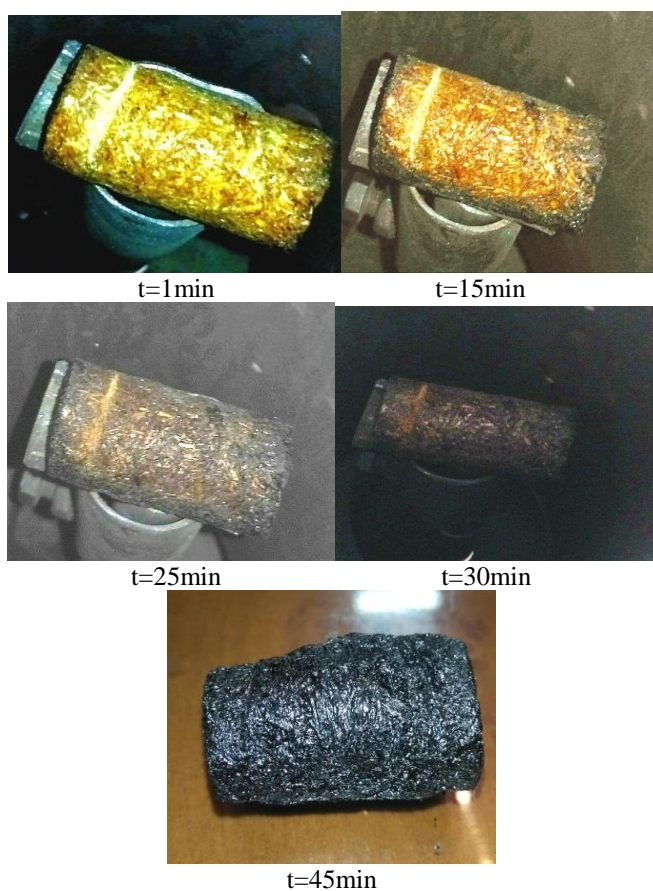


Figure 5. Combustion behavior of wheat dust pellet with time

Figure 5 shows the combustion behavior of wheat dust pellet with time. After the pellet exposed to the high temperature air in the combustor, the biomass pellet is heated up creating a rise in its surface temperature. Then, the heat is transferred from the pellet surface to its center in by conduction, where the conductivity of wheat dust pellet is a function of temperature and solid residues such as char and ash. As the time increases, the ignition behavior has an orange glowing appeared on the bottom pellet surface. This orange glowing observed may be attributed to heterogeneous ignition which is characterized by a direct attack of preheated air on the pellet. Bright and high temperature spots appear on the pellet surface as the time increases. The wheat dust pellet little by little becomes darkened and finally turned into char black and gray smoke was observed by the naked eye during the volatile matters releasing. Combustion at the pellet surface was noticed at the bottom surface of the pellet, but no visible flame appeared in the gas phase during any of the experiments due to the large stretch rate near to the stagnation region. It is shown in figure 5, as the pyrolysis process continues and volatiles releasing combustion proceed, the shape of the wheat dust pellet changes and the pellet was bending over itself in some cases. The physical properties of the produced pellet as porosity and surface area as well as the shape of the pellet char differ from those of the original pellet. The shape of the pellet char was observed more rounded than that of the original pellet because of the surface tension of the pellet that would let the pellet be partially melted or softened (deformed) during the combustion. Figures 6 (a-d), 7 (a-d) and 8 (a-d) illustrate the combustion behavior of wheat dust pellets at a different starting air temperature. During combustion, the particular components of biomass such as cellulose, hemicelluloses and lignin decompose to form water, light gases such as CO₂, CO, CH₄, and char. It is known that the biomass mainly composed of hemi-cellulose, cellulose and lignin, which decompose at different temperature ranges of 225–325°C, 305–375°C and 250–500°C, respectively [33]. Pellet ignition by means of the gaseous volatiles combustion also leads to a temperature increase in the pellet center. It can be seen from the figures that, after moisture evaporates at the beginning, the devolatilization and sudden rise in temperature happens in a short period of the total combustion time. Nearly 40-50% of the total energy was released during the volatile gas combustion, and its mass loss rate is a slow process resulting in longer periods of combustion before the formation of ash and this is matched with previous works [37–38]. As the quantity of volatiles released increases, the combustion process has improved. The char combustion does not occur on the surface of the pellet until the volatile combustion is nearly completed. Combustion process completion is signaled by a sudden decrease in the char temperature and no mass loss of fuel is noticed as shown in figures [6– 8]. The volatile matter combustion time is larger than that of the char combustion time where the combustion of volatile matters requires 70% of the total combustion process time, while the combustion of char requires about 15% of the total combustion process time. From the combustion behavior of the pellet at the surface and center, we can observe that the temperature inside the pellet is lower than that of the surface temperature with a gap ranged between 20 to 40°C at starting of ignition between them. This means that during the ignition; the temperature inside the pellet is still cold, the temperature distribution inside the pellet will be more constant and no reaction happens there yet, while the outside of the pellet can be high already. In this work, the

internal ignition temperature of biomass pellets was also measured and recorded. Although there is a certain temperature gradient with the particle surface, their temperature change trend is similar as reported in refs [39-42] who confirmed this phenomenon. The value of internal ignition temperature was obtained according to figure 9. The heterogeneous ignition theory also suggested that the internal ignition temperature depended on the starting air temperature [37].

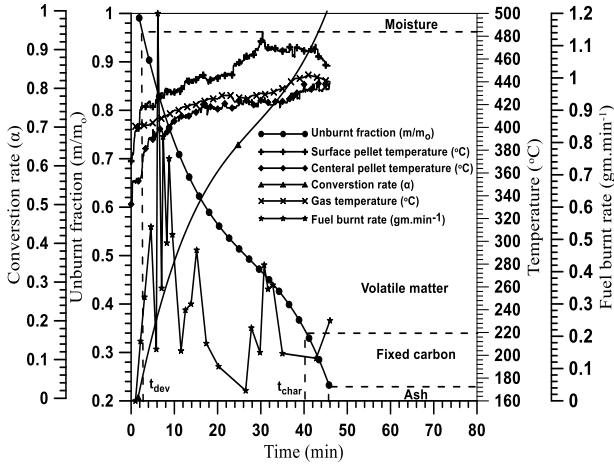


Figure 6a. Ignition behavior of wheat dust pellet D1 at 400°C

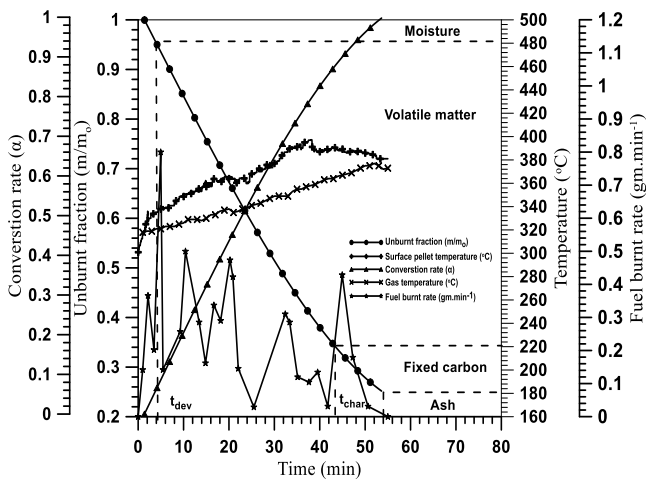


Figure 6b. Ignition behavior of wheat dust pellet D1 at 320°C

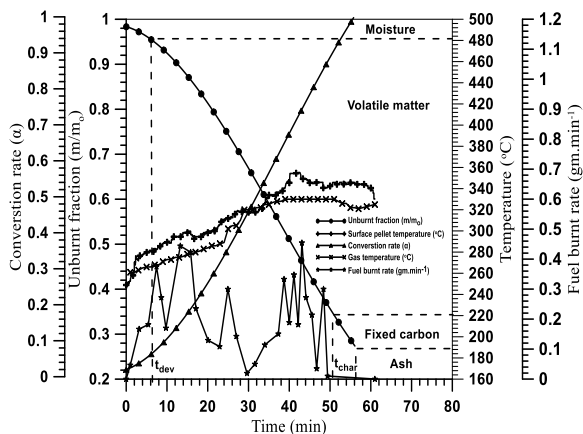


Figure 6c. Ignition behavior of wheat dust pellet D1 at 260°C

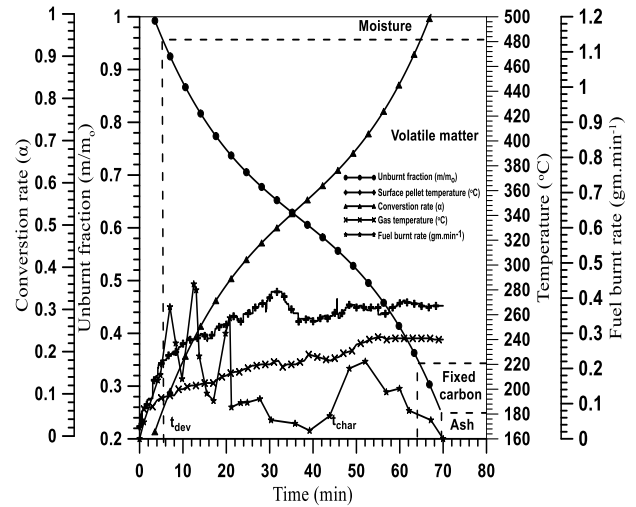


Figure 6d. Ignition behavior of wheat dust pellet D1 at 180°C

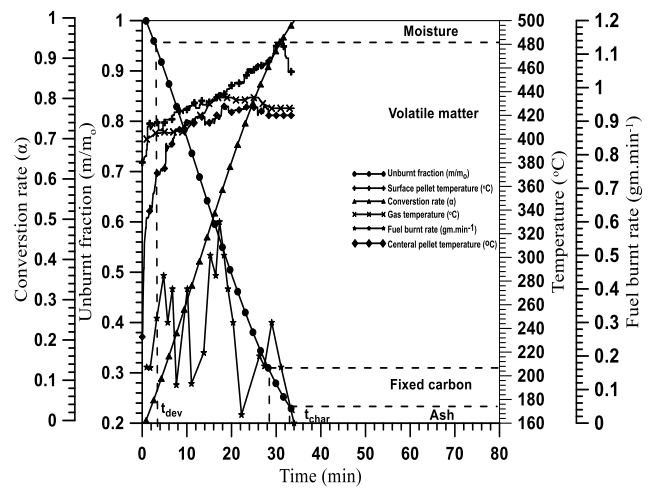


Figure 7a. Ignition behavior of wheat dust pellet D2 at 400°C

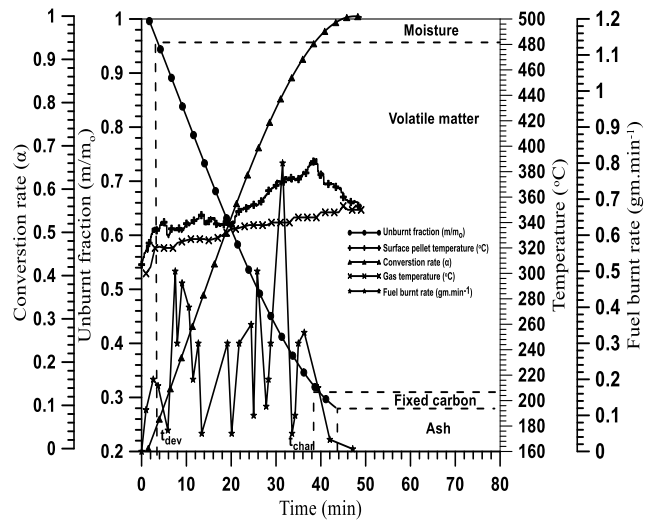


Figure 7b. Ignition behavior of wheat dust pellet D2 at 320°C

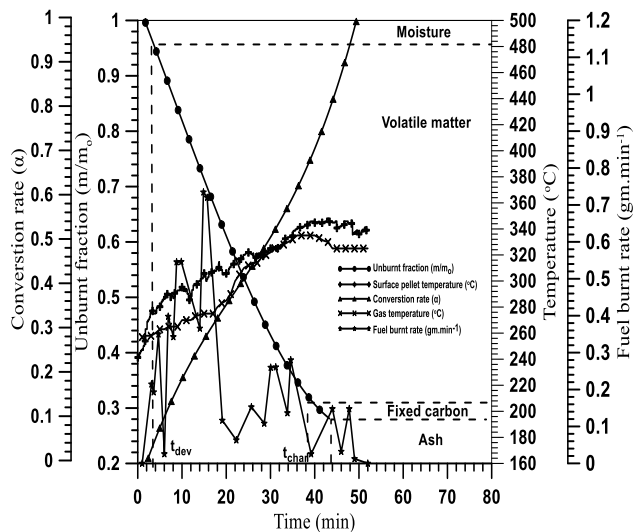


Figure 7c. Ignition behavior of wheat dust pellet D2 at 260°C

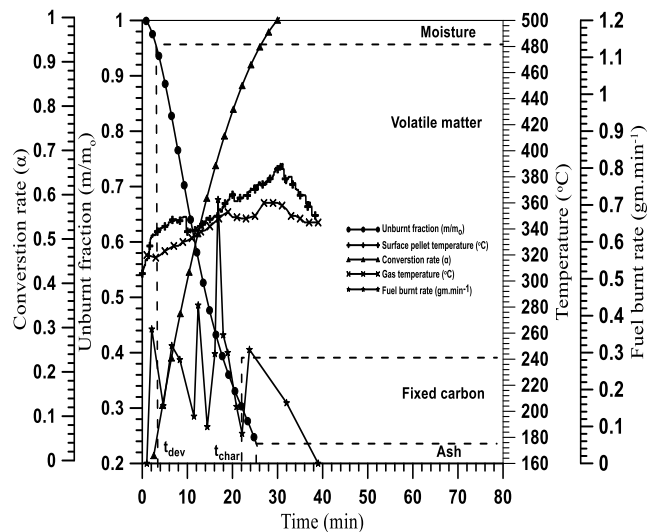


Figure 8b. Ignition behavior of wheat dust pellet D3 at 320°C

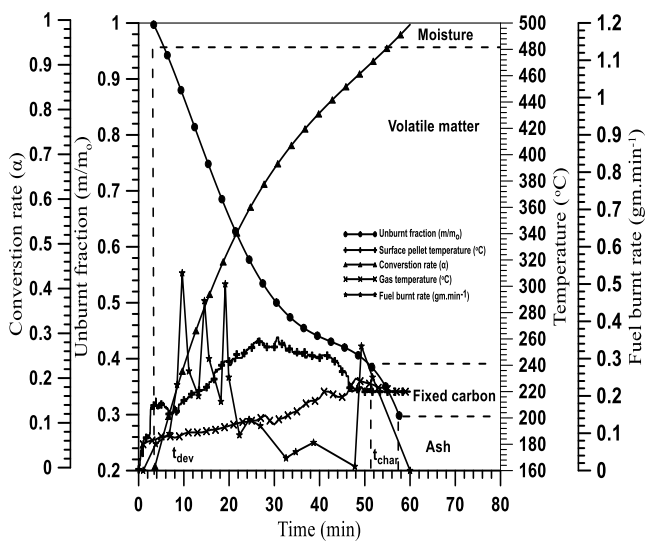


Figure 7d. Ignition behavior of wheat dust pellet D2 at 180°C

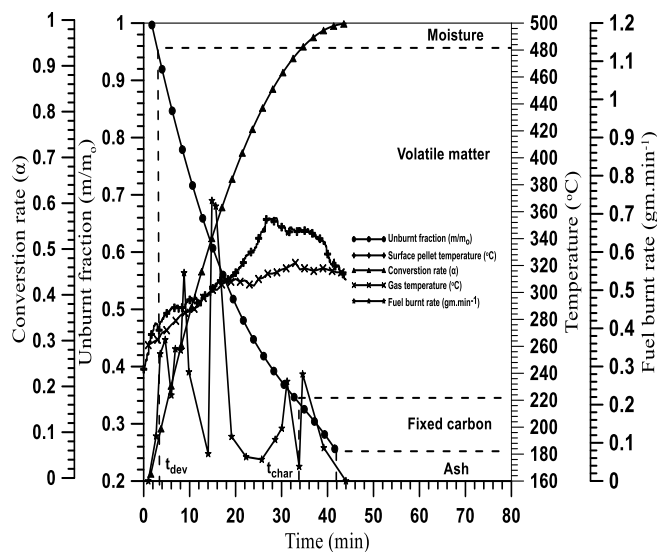


Figure 8c. Ignition behavior of wheat dust pellet D3 at 260°C

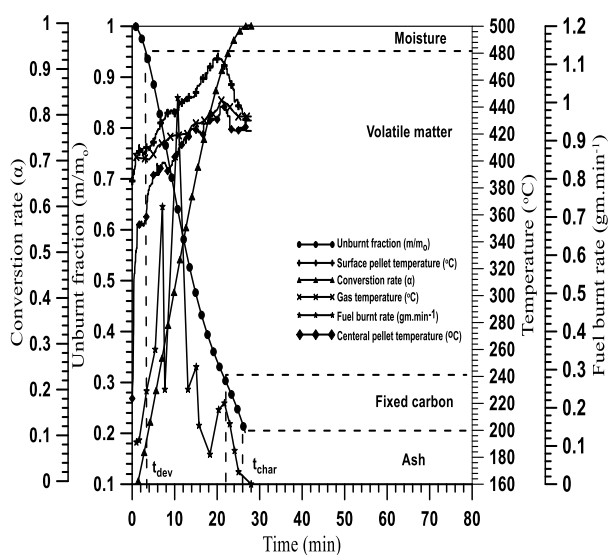


Figure 8a. Ignition behavior of wheat dust pellet D3 at 400°C

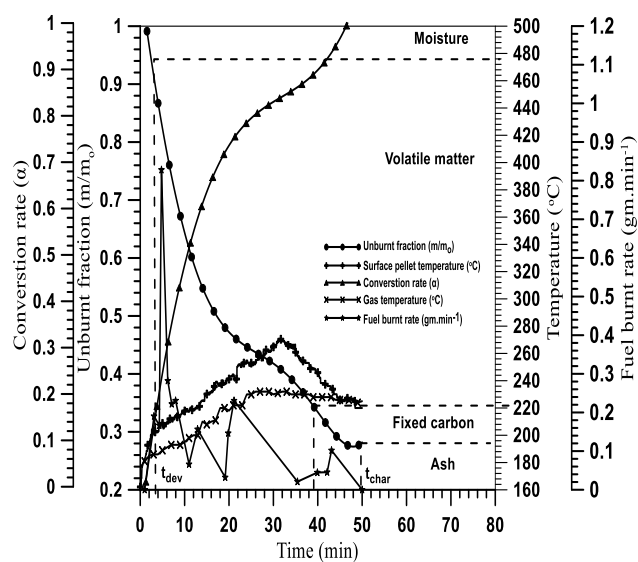


Figure 8d. Ignition behavior of wheat dust pellet D3 at 180°C

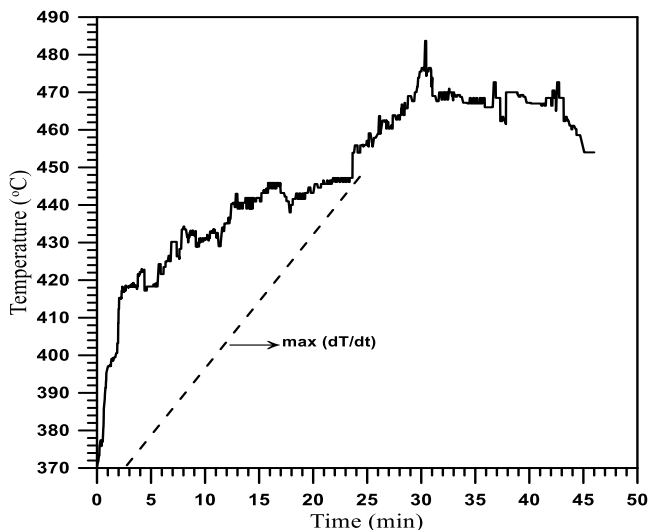


Figure 9. Temperature vs. time for internal ignition temperature determination

3.3 Effect of startup air temperature on combustion characteristics

Any slight increase in the temperature can greatly affect the ignition time since the heat transfer is an exponential function of temperature and a radiative heat flow is proportional to the (T^4). In the high air temperature [400°C and 320°C], the wheat dust pellet is heated for a short duration time for different sizes and shapes of pellets because the surface temperature rises rapidly and the conversion rate of the combustion process depends on the rates of the chemical reactions. As the starting air temperature increases, the rates of chemical reactions increase. On the other hand, in the low air temperatures [260°C and 180°C], the wheat dust pellet is heated for a long duration time for different sizes and shapes. The effect of starting air temperature on the combustion parameters of D1, D2 and D3 are shown in figures [10 (a, b and c)]. The pellet surface temperature is important during biomass combustion because it determines the amount of heat flux conducting from the pellet surface into its center, and so governs the drying and devolatilization processes along its radius [43]. As air temperature increased, the interior molecules gained sufficient kinetic energy that increased its velocity and broke chemical bonds, which in turn increased the frequency factor. So, the rate of collision and the chemical reaction rate increased. It is shown that as the starting air temperature increases from 180-400°C, a decrease in the devolatilization time is occurring for different sizes and shapes as shown in Table 5. Devolatilization proceeds less when the start up temperature increases, which may be referred to a more rapid internal heat transfer that increase the rate of devolatilization reactions [44]. Similar behavior was seen by [45] during combustion of coal and wood pellets. The results also showed that, increasing the starting air temperature from 180-400°C, leads to a reduction in char combustion time for different sizes and shapes. One can see that as the starting air temperature increases from 180°C to 400°C, the devolatilization temperatures during the combustion increase for different sizes and shapes as shown in Table 5. This behavior was expected, since the enhanced heat transfer due to the hotter surroundings accelerates the reaction rate of the combustion process. As the starting air temperature increases, the maximum combustion temperatures increase for different sizes and shapes as shown in Table 5. The maximum combustion temperature will affect on cellulose,

hemicelluloses and lignin composition. As the starting temperature increases, the time needed to reach the maximum temperature decreases from 45.57min to 30.37min for D1, from 44.8min to 30.75min for D2 and from 30.25min to 20.2min for D3. It is also noticed that as the starting air temperature increases, the ash temperatures of pellets during the combustion increase for different sizes and shapes as shown in Table 5. The ash temperature will effect on ash composition that will effect on fouling and slagging index. As the starting air temperature increases, the ash % decreases for different sizes and shapes as shown in Table 5. Moreover, ash can also has an important effect on pellet surface heat transfer and also affect the oxygen diffusion to the pellet surface during char combustion.

The results show that the rate of increase in the pellet surface temperature increases with increasing air starting temperature and the rate of mass loss rises shortly before ignition. This temperature rise reaches to 2-4% during the devolatilization stage where almost 70% of the pellet mass is converted to gas in a very low time period. The remaining char combustion process is still happening until the total biomass pellet conversion is accomplished and a sharp decrease in the production of combustible gases CO and CO₂ from the pellet is noticed. At air temperature 400°C, more rate of mass loss was recorded at the moment of ignition compared to other air temperatures and sometimes at this high temperature the pellet breaks down. The pellet overheats so quickly with high air temperature so that the volatiles emitted from the pellet surface are decomposed and the evaporation of these volatiles becomes possible from the deeper layers of the pellet [46-47]. In these experiments, the internal ignition temperature of biomass pellets was measured. From a comparison of the total combustion rate of D1, D2 and D3, we can notice that as the starting air temperature increases, the combustion rate increases from 1 to 1.61 ($\text{mg m}^{-2}\text{s}^{-1}$) for D1, from 1.62 to 3.12 ($\text{mg m}^{-2}\text{s}^{-1}$) for D2 and from 0.08-0.22 ($\text{mg m}^{-2}\text{s}^{-1}$) for D3. It can be noticed that the hexagonal pellet has the so lower combustion rate compared to the other pellets because of its geometry and the heat and flow conditions.

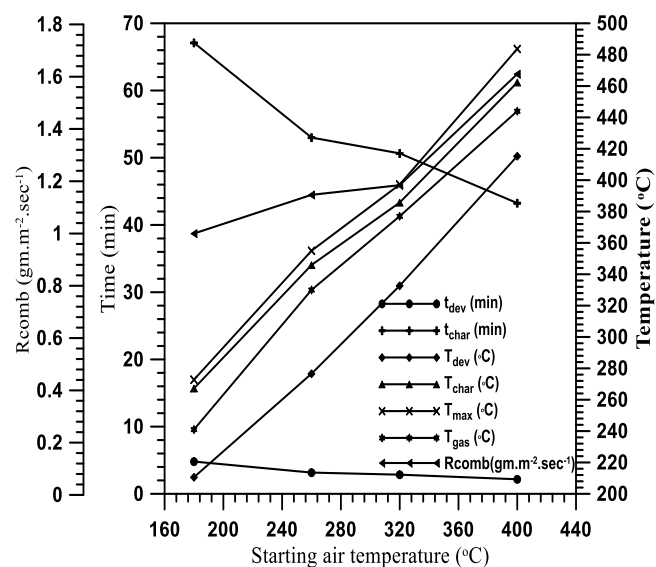


Figure 10a. The effect of starting air temperature on combustion parameters for D1

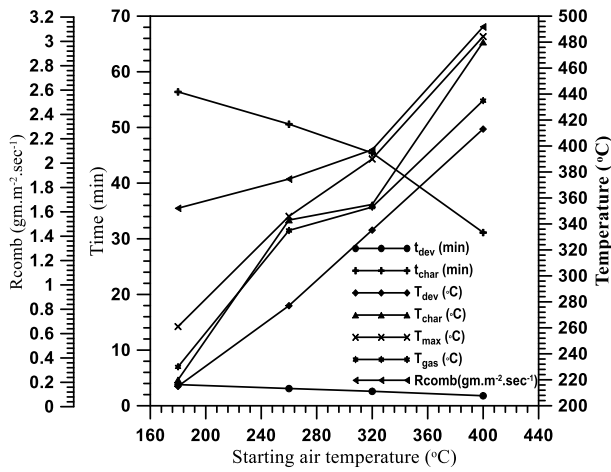


Figure 10b. The effect of starting air temperature on combustion parameters for D2

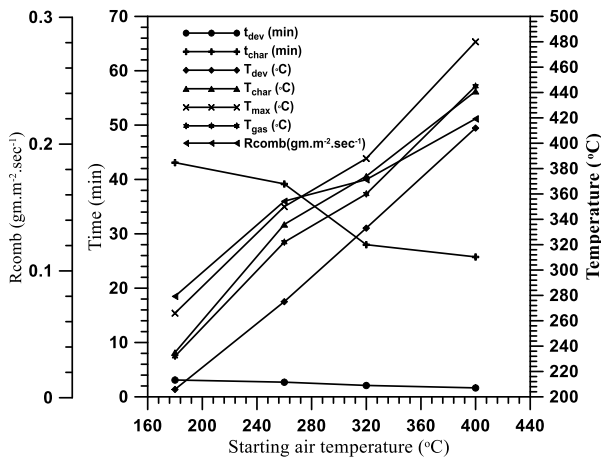


Figure 10c. The effect of starting air temperature on combustion parameters for D3

3.4 Effect of air velocity on the combustion characteristics

Figure 11 shows the effect of air velocity on the combustion process of the pellet D1 at 400°C. Heat is transmitted by two methods; conduction inside the pellet, convection and radiation from surrounding to the pellet surface. So, higher air velocities enhance both heat and mass transfer between air and pellet. When the air velocity becomes high, the heat transfer coefficient also becomes high and so the heat transfer monotonically increases. The results showed that in the high air velocity 4.2 m s⁻¹, the pellet heating process takes a short duration that reaches to 46 min. On the other hand, in the lower air velocity 3.2 m s⁻¹, the pellet heating process takes a long duration that reaches to 60 min. The increase in the primary air velocity from 3.2 to 4.2 m s⁻¹ leads to an increase in the combustion rate from 1.4 to 1.61 (mg m⁻² s⁻¹), respectively. The increase in air velocities leads to a reduction in the devolatilization time from 3.0 min at air velocity 3.2 m s⁻¹ to 2.3 min at air velocity 3.8 m s⁻¹ to 2.167 min at air velocity 4.2 m s⁻¹. The increase in air velocities leads to a reduction in the char time from 50 min at air velocity 3.2 m s⁻¹ to 46.6 min at air velocity 3.8 m s⁻¹ to 43.25 min at air velocity 4.2 m s⁻¹. Devolatilization and char proceeds less when the air velocity increases, which may be referred to a more rapid internal heat transfer because the heat transfer coefficient is high that increase the rate of devolatilization and char reactions. As the

air velocity increases, the devolatilization temperature increases from 408.7°C ±1.1°C to 415.3°C±1.12°C and the maximum temperature increases from 470.3°C±1.2°C to 483.7°C±1.2°C. The amount of volatiles evaporating from pellets increases as the air velocity increases and the amount of combustion ash decreases from 27.3%±0.69% at air velocity 3.2 m s⁻¹ to 25.8%±0.66% at air velocity 3.8 m s⁻¹ to 23.7%±0.97% at air velocity 4.2 m s⁻¹. Increases in air velocity lead to a decreasing in combustion times, char combustion times, fuel ignition temperatures and the amount of ash while the amount of volatiles evaporating from pellets and combustion rate increase. This results are matched with other works [48,41].

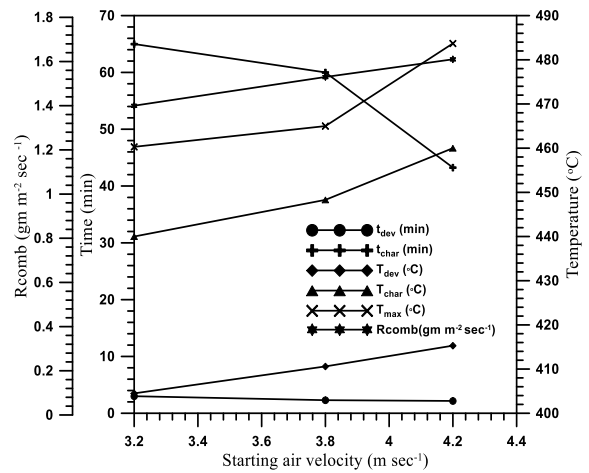


Figure 11. The effect of starting air velocity on combustion parameters

3.5 Effect of pellet size on the combustion characteristics

The pellet shape and size have a considerable effect on conduction, convection and radiation heat transfer mechanisms and on the char combustion and ash formation rate as shown in refs. [42,49-52]. As shown in the previous work, the pellet size may affect the thermal history of the biomass pellet [53-54]. At the beginning of devolatilization process, small sizes are completely dried compared to larger sizes, which still contain some moisture. Since devolatilization rate is affected by the amount of heat transferred to the pellet, the remaining moisture in the larger sizes slows the heat transfer within them. So the intensity of devolatilization is greater for smaller sizes and volatiles are released from small sizes at a higher rate. For small sizes, the combustion stages as drying, devolatilization, and char burning occur sequentially, while for larger sizes, there is an overlap between drying and devolatilization stages. The effect of pellet size on the ignition behavior of the wheat dust pellet at a different starting air temperature was experimentally investigated. As shown in table 5 at the high diameter D1, the wheat dust pellet is heated for a long duration time. On the other hand, in the small diameter D3, the wheat dust pellet is heated for a short duration time as the heat transfer resistance increases with the increase in pellet diameter. The decrease in diameter of pellets from 18 to 6 mm leads to a reduction in the devolatilization time at the different startup air temperatures. The decrease in diameter of pellets from 18 to 6 mm leads to reduction in char time at the different startup air temperatures. Devolatilization and char proceed less when the diameter of pellet decreases, which may be referred to a more rapid internal heat transfer which

increases the rate of devolatilization and char reactions. The produced char also depends on the size; it becomes higher for larger pellets compared to the smaller pellets. The decrease in diameter of pellets from 18 to 6 mm leads to a reduction in % ash at the different startup air temperatures. This behavior was expected, since the enhanced heat transfer for pellet lower diameters accelerates reaction rate of the combustion process. Correlations between the input parameters such as starting air temperature, pellet size, and the combustion parameters such as ignition time, ignition temperature, char time and char temperature as given in eqs. (19-22) with the aid of the data fit are obtained as shown in figures 12 (a-d); where $D/L = (18/42)$ to $(6/42)$ and $T_{st} = 180$ to 400 °C are:

$$t_{dev}^* = 0.013T_{st}^* + 0.076300 \left(\frac{D}{L}\right)^2 \quad R^2=0.96 \quad (19)$$

$$t_{char}^* = 0.418T_{st}^* - 0.15170 \left(\frac{D}{L}\right)^2 \quad R^2=0.97 \quad (20)$$

$$T_{dev}^* = 0.4268T_{st}^* - 0.09343 \left(\frac{D}{L}\right)^2 \quad R^2=0.94 \quad (21)$$

$$T_{char}^* = 0.4632T_{st}^* + 0.5390 \left(\frac{D}{L}\right)^2 \quad R^2=0.92 \quad (22)$$

where $t_{dev}^* = \frac{t_{dev}}{t_{total}}$, $t_{char}^* = \frac{t_{char}}{t_{total}}$, $T_{dev}^* = \frac{T_{dev}}{T_{max}}$, $T_{char}^* = \frac{T_{char}}{T_{max}}$, $T_{st}^* = \frac{T_{starting\ K}}{300K}$

From these analyses we can obtain the following important observations: (a) the pellet size effects the combustion process more than the pellet composition itself, (b) a pellet thick heated layer is established with the low air temperature because of long heating time, whereas a pellet thin heated layer is established with the high air temperature because of a quick heating (short period), (c) increases in air velocity leads to a reduction in combustion time, char combustion time, and an increasing in ignition temperature and peak temperature, and (d) Regarding to environment aspects and residence time required for pellet combustion, optimization conditions of the combustion process is required. Considering that lowest ignition temperature, lowest pellet surface temperature, shortest ignition time, and longer time required for the combustion process were selected, hexagonal pellet is the best shape of combustion according to these conditions in this study.

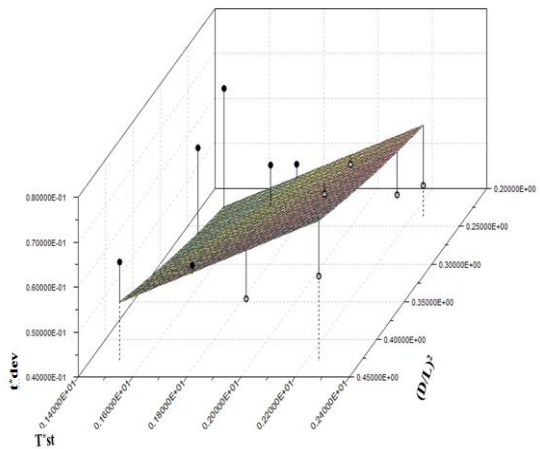


Figure 12a. The effect of operating conditions on devolatilization time

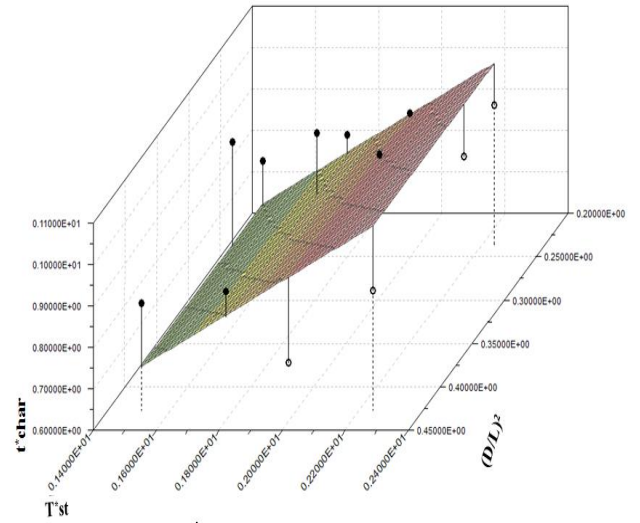


Figure 12b. The effect of operating conditions on char time

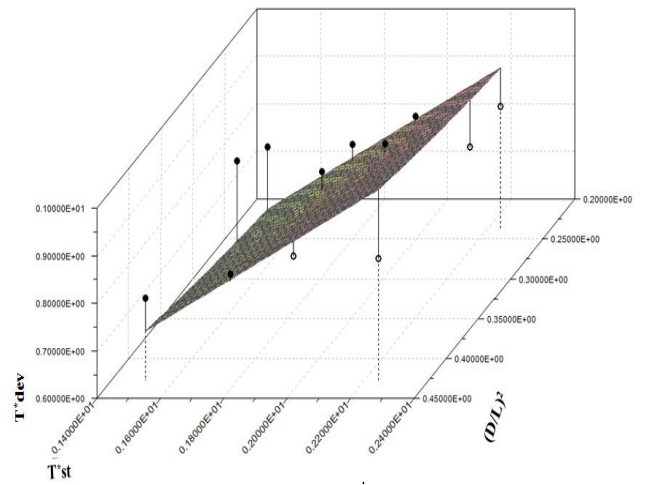


Figure 12c. The effect of operating conditions on devolatilization temperature

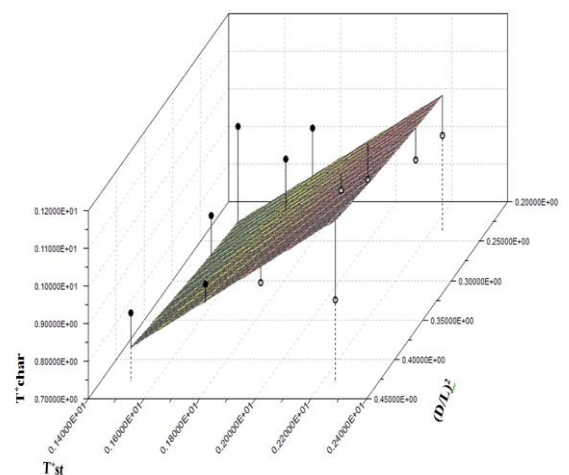


Figure 12d. The effect of operating conditions on char temperature

3.6 Correlations of ignition time and ignition temperature using analytical solutions

Coupling of the mathematical model and numerical

simulation is used to earning a better understanding of the thermal decomposition of biomass pellet in a fixed-bed combustor. Considering that the mass loss rate before pellet ignition is the summation of the pyrolysis rate and the evaporation of moisture rate, the mass loss rate equation can be put in the following form:

$$\frac{\partial \rho_s}{\partial t} = \dot{r}_p + \dot{r}_m = -(\rho_s - \rho_c)A_p \exp\left(-\frac{E_p}{RT_s}\right) - \delta(r - R_m) \frac{dR_m}{dt} \rho_s C_m \quad (23)$$

The rate of pyrolysis \dot{r}_p is described by a first order step with Arrhenius kinetics. The char's density, ρ_c , is set to be $0.2\rho_s$. The rate of evaporation of moisture, \dot{r}_m , is written in the form used in [4]. R_m is the radius of evaporation front, $\delta(r - R_m)$ is the Dirac delta function, and C_m is the moisture content. The energy balance for the solid fuel can be described generally as follows:

$$\rho_s c_{p_s} \frac{\partial T_s}{\partial t} = \frac{1}{r^2} \frac{\partial(k_s r^2 \frac{\partial T_s}{\partial r})}{\partial r} - G_g \frac{\partial \Delta h_g}{\partial r} - \dot{r}_p \Delta h_p - \dot{r}_m \Delta h_m \quad (24)$$

where: Δh_p and Δh_m in Eq. (24) are the pyrolysis and evaporation of water heats, respectively. The Δh_g is the volatile matter average enthalpy. Assuming a thermal equilibrium between the gas and the solid inside the pellet and ignition usually occurs on the pellet lower half that facing the hot air, Eq. (24) is considered as a one-dimensional energy balance of a pellet. A one-dimensional model may be used along the cylindrical combustors centerline, however, different assumptions have been considered during the modeling process. These common simplifications are: (a) The solid phase is considered as a homogeneous medium; (b) All solid fuels consist of: water, moisture, volatiles, char and ash; (c) Gas flow is incompressible and the fuel and gases are idealized as a plug flow; (d) Pressure drop along the bed can be neglected. Considering that the gas can only flow in the vertical direction and the one-dimensional conduction of heat in a semi infinite solid exposed to the heat flux, q'' , gives an ignition time in the following form [55]:

$$t_{ig,theoretical,1} = \frac{\pi}{4} k_s \rho_s c_{p_s} \left(\frac{T_{ig}-T_0}{\varepsilon q''}\right)^2 \quad (25)$$

where $t_{ig,theoretical,1}$: theoretical ignition time (sec), k_s : solid thermal conductivity ($\text{kWm}^{-1}\text{K}^{-1}$), ρ_s : Solid density (kg m^{-3}), ε : emissivity, T_{ig} : ignition temperature $^{\circ}\text{C}$, T_0 : ambient temperature $^{\circ}\text{C}$ and q'' : heat flux kW m^{-2} . The heat of pyrolysis and the pellet size effect are ignored in Equation (25). For a single pellet ignited in a hot air stream a heat flux $q'' = h(T_a - T_0)$. The predictions obtained from the present model are in a good agreement with the experimental results of the surface pellet temperature measurements, but failed to predict correctly the experimental results of the center pellet temperature measurements. Pyrolysis rates for biofuels have been studied extensively, and numerous models have been constructed. Of particular interest are the data developed by ref. [56], where the total pyrolysis time as a function of pellet diameter and pyrolysis temperature is given in the following form:

$$t_{ig,theoretical,2} = 421.5 + (0.779 \times D^2) - (0.457 \times T) \quad (26)$$

where $t_{ig,theoretical,2}$ is expressed in seconds, D is pellet

diameter expressed in millimeters (mm), T is pyrolysis temperature expressed in $^{\circ}\text{C}$, the coefficient of determination (R^2) associated with equation (26) is 0.93. The predictions obtained with $t_{ig,theoretical,2}$ are in a good agreement with the experimental results of small size pellet and high air temperature, but failed to predict correctly the experimental results of pellet (D1) and low air temperature as shown in figure 13.

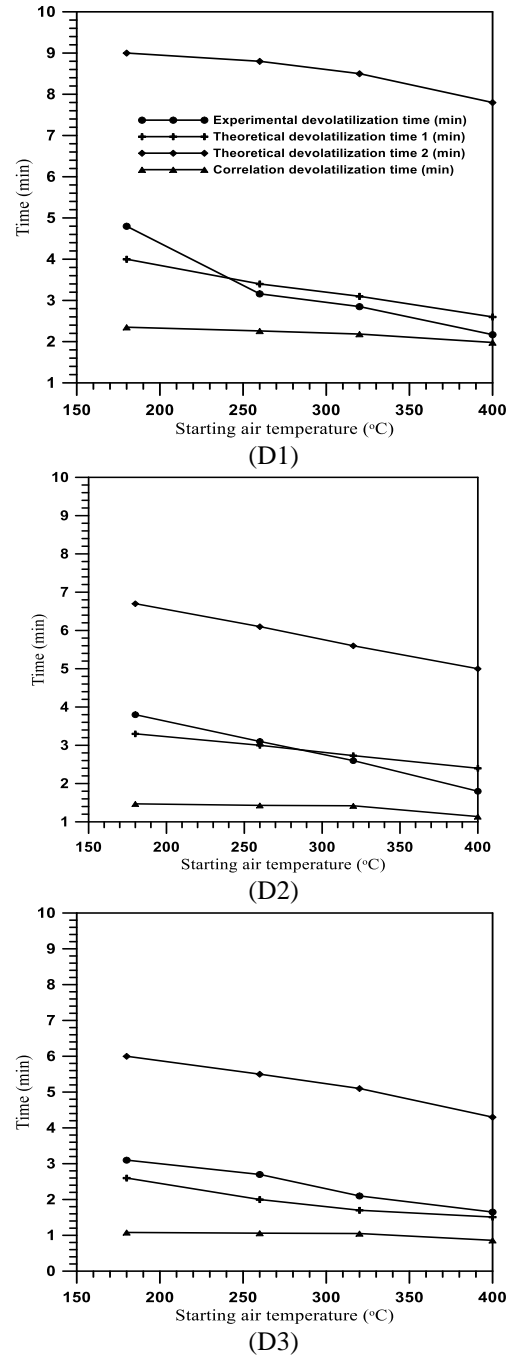


Figure 13. Comparison between the ignition time from the present experimental work and theoretical models correlations for D1, D2 and D3

3.7 The gaseous emissions

Figures 14 (a-c) show the emissions from the combustion of wheat dust pellet in the fixed bed combustor. The combustion reaction starts after fuel drying and condenses gradually after

3 min; accordingly, CO and CO₂ concentration increases, and reaches their maximum values after about 30 to 40min. The CO₂ formation at low temperatures was mainly due to the cracking and reforming of C=O and COOH functional groups, but the formation of CO may be due to the cracking of carbonyl (C-O-C) and carboxyl (C=O) groups [10]. Since the biomass ignition temperature is low, the devolatilization process leads to incomplete combustion and increased pollutant emissions. Most emissions from the ignition and combustion of wheat dust pellet depend on the starting air temperature, the air velocities and pellet diameter. The emissions of wheat dust pellet at different operating conditions are given in Figures 14(a-c). As shown in figure 15, as the air temperature that enters the combustor increases, the values of surface pellet temperature increase. This increasing in temperature, led to an increase in the amount of CO₂ due to complete combustion that reached its maximum value about 20.3 vol.% ±0.49% at 400°C for all sizes. Because the temperature is high enough to let the evolved CO reacts with oxygen to form CO₂. The increase in the amount of CO₂ and the decrease of CO may be occurring because the rate of collision and the chemical reaction rate increased with increasing the bed temperature and this is can be concluded from the oxygen concentration reduction in that region. As the heating time increases, the CO concentration increases from 11 ppm to 35ppm for D1, from 13ppm to 60ppm for D2 and from 0 ppm to 15ppm for D3. The trend of the gas emissions is matched with the work done in refs. [57-58]. The sulfur content in the composition of the materials is traced, so the concentration of SO₂ and H₂S is also traced.

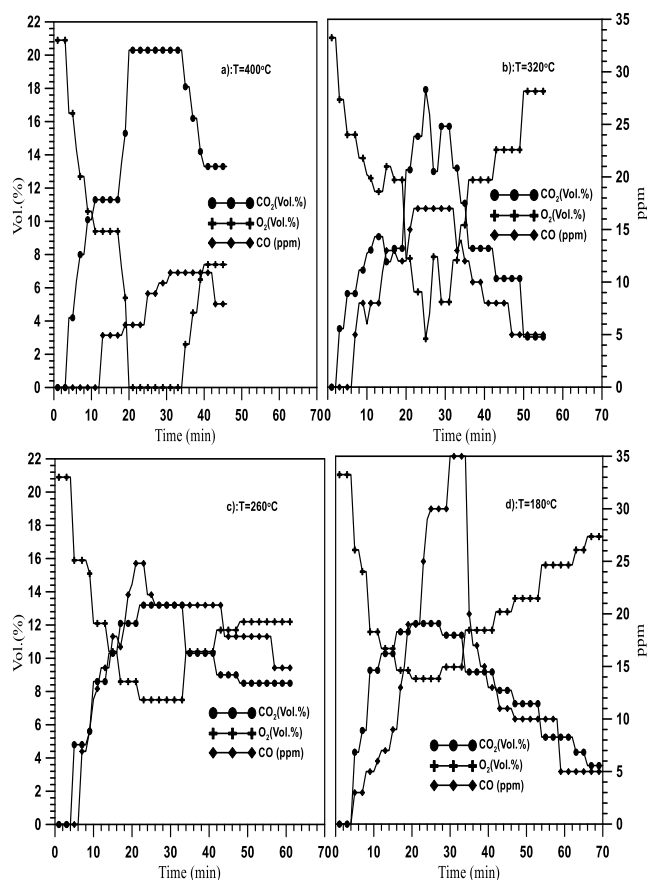


Figure 14a. The emissions from the combustion of wheat dust pellet for D1 at different temperature (a) T=400°C, (b) T=320°C, (c) T=260°C and (d) T=180°C

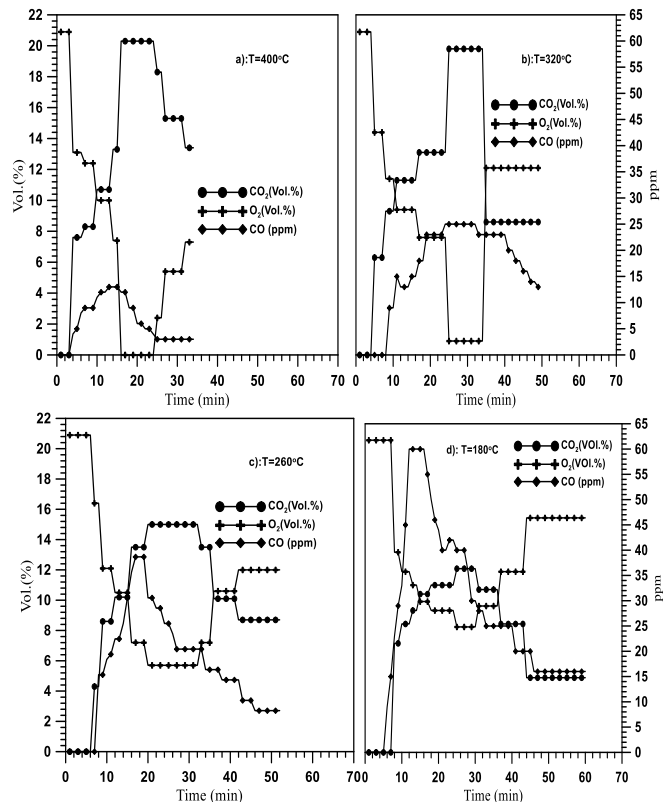


Figure 14b. The emissions from the combustion of wheat dust pellet for D2 at different temperature (a) T=400°C, (b) T=320°C, (c) T=260°C and (d) T=180°C

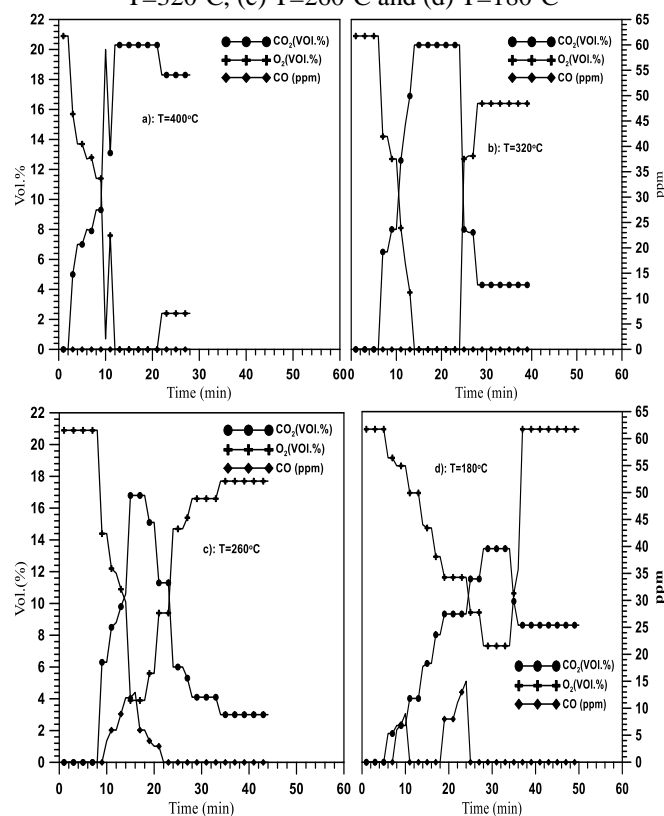


Figure 14c. The emissions from the combustion of wheat dust pellet for D3 at different temperature (a) T=400°C, (b) T=320°C, (c) T=260°C and (d) T=180°C

The CO and CO₂ emissions concentration percentage can be used to evaluate the combustion efficiency of biomass pellets inside the fixed bed combustors, so the combustion efficiency

of the combustion process under different operating conditions inside the combustor can be determined from the following equation:

$$\eta_c = \frac{CO_2(\%)}{CO(\%)+CO_2(\%)} \quad (27)$$

However, η_c is not sensitive to low CO concentrations, which are usually in the combustion processes that are typically involved in this type of experiments. It was found that the combustion efficiency ranged between 99% and 100% and it reaches to 100% in some experiments. As discussed before, the surface pellet temperature increases with increasing the air temperature. This increased in the pellet temperature increased the amount of CO₂, but decreased the amount of CO produced. According to these obtained values of CO₂ and CO, the combustion efficiency increased. The results indicate that hexagonal pellets burn quickly in the combustion chamber leading to a high combustion efficiency and leads to highest CO₂ concentration. In contrast, D1 for wheat dust pellets have the highest CO concentration of 60 ppm at 180°C and 8.7% O₂.

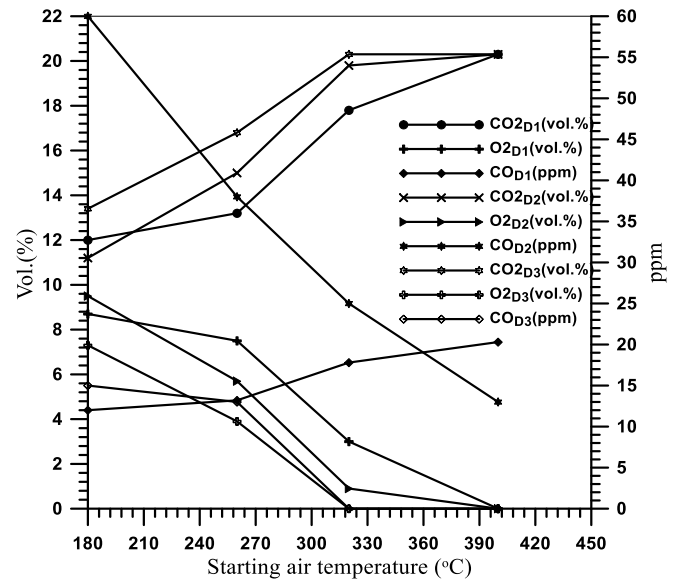


Figure 15. The effect of starting air temperature on emission parameters for D1, D2 and D3

Table 5. Effect of starting air temperature and die size on the combustion parameters

Die size	D1				D2				D3			
	400°C	320°C	260°C	180°C	400°C	320°C	260°C	180°C	400°C	320°C	260°C	180°C
Temp.	400°C	320°C	260°C	180°C	400°C	320°C	260°C	180°C	400°C	320°C	260°C	180°C
t _{dev} (min)	2.17	2.85	3.16	4.8	1.8	2.6	3.1	3.8	1.65	2.1	2.7	3.1
t _{ig,theoretical1} (min)	2.6	3.1	3.4	4	2.4	2.73	3	3.3	1.51	1.7	2	2.6
t _{ig,theoretical,2} (min)	7.8	8.5	8.8	9	5	5.6	6.1	6.7	4.3	5.1	5.5	6
T _{dev} °C	415.3±	332.7±	276.6±	210.8±	413.1±	335.3±	277.1±	215±	412±	333.1±	275.1±	205.9±
	1.11 °C	1.03 °C	0.97 °C	0.91 °C	1.11 °C	1.03 °C	0.97 °C	0.92 °C	1.11 °C	1.03 °C	0.97 °C	0.9 °C
t _{char} (min)	43.25	50.65	53	67.1	31.13	45.13	50.6	56.4	25.75	28	39.18	43.1
t _{intignition} (min)	3	4.3	4.8	5.2	2.6	2.9	3.3	4	2	2.5	3	3.3
T _{char} °C	462.3±	385.7±	345.9±	267.2±	480±	355±	343.1±	220±	441±	374±	336±	235±
	1.16 °C	1.09 °C	1.04 °C	0.98 °C	1.18 °C	1.04 °C	1.04 °C	0.92 °C	1.14 °C	1.07 °C	1.03 °C	0.94 °C
T _{max} °C	483.7±	397.2±	355±	272.8±	484.3±	390±	345.9±	261±	480±	388±	350±	266±
	1.18 °C	1.1 °C	1.05 °C	0.97 °C	1.18 °C	1.09 °C	1.04 °C	0.96 °C	1.18 °C	1.08 °C	1.05 °C	0.96 °C
t _{Tmax} (min)	30.37	38.05	42.63	45.57	30.75	38.53	44.8	30.55	20.2	30.25	28.5	30.25
α _{dev} %	4	3.33	2.91	2.22	3.9	3.8	3.6	2.5	5.5	3.3	2.2	1.1
α _{char} %	96.116	95	93.3	90.56	98.73	93.5	90.9	88.9	98.1	96.8	96	91.66
Ash%	23.7±	25±	27.97±	29.57±	21.14±	24.7±	28±	29.53±	20±	23.75±	25.3±	28±
	0.97%	0.96%	0.63%	0.57%	1.9%	1.37%	1.114%	0.98%	5.1%	2.8%	2.27%	5.1%
R _{comb} (g/m ² s)	1.61	1.185	1.148	1	3.12	2.11	1.87	1.62	0.22	0.172	0.155	0.08
T _g °C	444	377	330	241	435	353	35	230	445	360	322	232
CO ₂ vol%	20.3±	17.8±	13.2±	12±	20.3±	19.8±	15±	11.2±	20.3±	20.3±	16.8±	13.4±
	0.5%	0.56%	0.75%	0.83%	0.5%	0.51%	0.67%	0.9%	0.5%	0.5%	0.6%	0.75%
O ₂ vol%	0±	3±	7.5±	8.7±	0±	0.9±	5.7±	9.5±	0±	0±	3.9±	7.3±
	0%	3.3%	1.3%	1.19%	0%	11.1%	1.75%	1.05%	0%	0%	2.56%	1.37%
Co ppm	11	17	25	35	13	25	38	60	0	0	13	15
t _{combustion} (min)	46	55	61	70	34	49	52	60	28	39	44	50

4. CONCLUSIONS

Combustion of wheat dust pellets of different sizes in a fixed bed combustor was studied under different operating conditions such as air temperature, pellet size and air velocity and the following conclusions can be derived as follows:

- Wheat dust pellet has lower activation energy and pre-exponential compared to the values of epoxy 1092.
- The ignition time, the maximum combustion rate time and burnt temperature of epoxy 1092 are lower than those of wheat dust pellet. The ignition index,

burnt index and activation energy of epoxy 1092 are higher than those of wheat dust pellet.

- As air temperature and air velocity increases, the combustion rate increases and devolatilization and char times decrease.
- The decrease in diameter of pellets from 18 mm to 6 mm, leads to an increase in the combustion rate and a decrease in devolatilization and char times.
- It was concluded from the results that, a hexagonal pellet is the best shape for combustion under the investigated conditions and parameters due to its lowest ignition temperature, lowest surface temperature, shortest ignition time, and longest time required for combustion.
- The predictions obtained from mathematical models are in good agreement with the experimental results of pellet surface temperature measurements, but failed to predict correctly the experimental results at the pellet center temperature measurements.
- The formation of CO₂ increases with increasing the air temperature and air velocity inside the combustor.
- It was found that the combustion efficiency ranged between 99% and 100%.
- The slagging index value of wheat dust pellets is 0.72 which indicates that this material has a medium slagging tendency and regarding to the fouling inclination, wheat dust pellet can be classified as a relatively high fouling inclination fuel.

REFERENCES

- [1] Saxena SC, Jotshi CK. (1994). Fluidized-bed incineration of waste materials. *Prog Energy Combust Sci* 20: 281-324. [https://doi.org/10.1016/0360-1285\(94\)90012-4](https://doi.org/10.1016/0360-1285(94)90012-4)
- [2] Biswas AK. (2014). Effect of pelletizing conditions on combustion behaviour of single wood pellet. *Appl Energy* 119: 79-84. <https://doi.org/10.1016/j.apenergy.2013.12.070>
- [3] Kung H. (1972). A mathematical model of wood pyrolysis. *Combustion and Flame* 18: 185-195. [https://doi.org/10.1016/S0010-2180\(72\)80134-2](https://doi.org/10.1016/S0010-2180(72)80134-2)
- [4] Saastamoinen J, Richard J. (1996). Simultaneous drying and pyrolysis of solid fuel particles. *Comb. Flame* 106: 288-300. [https://doi.org/10.1016/0010-2180\(96\)00001-6](https://doi.org/10.1016/0010-2180(96)00001-6)
- [5] Saastamoinen J, Taipale R, Horttanainen M, Sarkomaa P. (2000). Propagation of the ignition front in beds of wood particles. *Combust Flame* 214-226. [https://doi.org/10.1016/S0010-2180\(00\)00144-9](https://doi.org/10.1016/S0010-2180(00)00144-9)
- [6] Ronnback M, Axell M, Gustavsson L. (2000). Combustion processes in a biomass fuel bed-experimental results. *Progress in Thermochemical Biomass Conversion*. 17-22. <https://doi.org/10.1002/9780470694954.ch59>
- [7] Fleckl T, Obernberger I, Jager H. (2000). Combustion diagnostics at a biomass-fired grate furnace using FT-IR absorption spectroscopy for hot gas measurements. In: *Proceedings of the 5th International Conference of Industrial. Portugal*.
- [8] Tissari J, Hytonen K, Lyyranen J, Jokiniemi J. (2007). A novel field measurement method for determining fine particle and gas emissions from residential wood combustion. *Atmos Environ* 41: 8330-8344. <https://doi.org/10.1016/j.atmosenv.2007.06.018>
- [9] Boman C, Israelsson S, Öhman M, Sweden L. (2008). Combustion properties and environmental performance during small scale combustion of pelletized hardwood raw material of aspen. In: *Proceedings of World Bioenergy, Jonkoping, Sweden*, pp. 27–29.
- [10] Kuo JT, Hsi CL. (2005). Pyrolysis and ignition of single wooden spheres heated in high temperature streams of air. *Combust Flame* 142: 401–412. <https://doi.org/10.1016/j.combustflame.2005.04.002>
- [11] Kraiem N, Jeguirim M, Limousy L, Lajili S, Dorge L, Michelin R. (2014). Mpregnation of olive mill wastewater on dry biomasses: Impact on chemical properties and combustion performances. *Energy* 78: 479-489. <https://doi.org/10.1016/j.energy.2014.10.035>
- [12] Khodaei H, Al-Abdeli YM, Guzzomi F, Yeoh GH. (2015). Overview of processes and considerations in the modelling of fixed-bed biomass combustion. *Energy* 88: 946-972. <https://doi.org/10.1016/j.energy.2015.05.099>
- [13] El-Sayed SA, Khairy M. (2015). Effect of heating rate on the chemical kinetics of different biomass pyrolysis materials. *Biofuels* 6: 157-170. <https://doi.org/10.1080/17597269.2015.1065590>
- [14] Nimmo W, Daood SS, Gibbs BM. (2010). The effect of O₂ enrichment on NO_x formation in biomass co-fired pulverized coal combustion. *Fuel* 89: 2945–2952. <https://doi.org/10.1016/j.fuel.2009.12.004>
- [15] Lajili M, Jeguirim M. (2014). Physico-chemical properties and thermal degradation characteristics of agropellets from olive mill by-products/sawdust blends. *Fuel processing Technology* 126: 215-221. <https://doi.org/10.1016/j.fuproc.2014.05.007>
- [16] Munir S, Daood SS, Nimmo W, Cunliffe AM, Gibbs BM. (2009). Thermal analysis and devolatilization kinetics of cotton stalk, sugar cane bagasse and shea meal under nitrogen and air atmosphere. *Bioresource Technology* 100: 1413–1418. <https://doi.org/10.1016/j.biortech.2008.07.065>
- [17] Fleckl T, Obernberger I, Jager H. (2000). Combustion diagnostics at a biomass-fired grate furnace using FT-IR absorption spectroscopy for hot gas measurements. In: *Proceedings of the 5th International Conference of Industrial Furnaces and Boilers. Portugal*.
- [18] Tissari J, Hytonen K, Lyyr anen J, Jokiniemi J. (2007). A novel field measurement method for determining fine particle and gas emissions from residential wood combustion. *Atmos Environ* 41: 8330-8344. <https://doi.org/10.1016/j.atmosenv.2007.06.018>
- [19] Wiinikka H, Gebart R. (2005). The influence of fuel type on particle emissions in combustion of biomass pellets. *Combust Sci Technol* 17741-63. <https://doi.org/10.1080/00102200590917257>
- [20] Bovy P. (2008). Effect of air preheating in moving grate furnaces: Modeling convective drying and experimental investigation of spontaneous ignition. PhD thesis. Eindhoven University of Technology, the Netherlands.
- [21] Pronobis M. (2005). Evaluation of the influence of biomass co-combustion on boiler furnace slagging by means of fusibility correlations. *Biomass Bioenergy* 28: 375–383. <https://doi.org/10.1016/j.biombioe.2004.11.003>
- [22] Song JH. (2013). Study on air preheater corrosion problem of CFB biomass directed-fired boiler in

- Zhanjiang biomass power plant. *Appl Mech Mater* 9291-294.
<https://doi.org/10.4028/www.scientific.net/AMM.291-294.294>
- [23] Amir MK, et. al. (2014). Corrosion prevention in boilers by using energy audit consideration. *Appl. Mech. Mater* 7–10.
<https://doi.org/10.4028/www.scientific.net/AMM.532.307>
- [24] Niu S, Han K, Lu C. Release of sulfur dioxide and nitric oxide and characteristic of coal combustion under the effect of calcium based organic compounds. *Chem. Eng. J.* 168 (2011) 255–261.
<https://doi.org/10.1016/j.cej.2010.10.082>
- [25] Li X, Ma B, Xu L, Hu Z, Wang X. Thermogravimetric analysis of the co-combustion of the blends with high ash coal and waste tyres. *Thermochimica Acta* 441(2006) 79–83. <https://doi.org/10.1016/j.tca.2005.11.044>
- [26] Gong X, Guo Z, Wang Z. Reactivity of pulverized coals during combustion catalyzed by CeO₂ and Fe₂O₃. *Combust. Flame* 157(2010): 351–356.
<https://doi.org/10.1016/j.combustflame.2009.06.025>
- [27] Arranz J.I., Miranda M.T., Montero I., Seplveda F.J., Rojas (2015) Characterization and combustion behavior of commercial and experimental wood pellets in South West Europe *Fuel* 142 199–207.
<https://doi.org/10.1016/j.fuel.2014.10.059>
- [28] Luo SY, Xiao B, Hu ZQ, Liu SM, Guan YW (2009). Experimental study on oxygen-enriched combustion of biomass micro fuel. *Energy* 34:1880–1884.
<https://doi.org/10.1016/j.biombioe.2004.11.003>
- [29] Coats, A.W., Redfern, J.P., (1964). Kinetic parameters from thermogravimetric data. *Nature* 201:68–69.
<https://doi.org/10.1038/201068a0>
- [30] Ahn H.K., Sauer T.J., Richard T.L., T.D. Glanville. Determination of thermal properties of composting bulking materials. *Bioresource Technology* 100: 3974–3981. <https://doi.org/10.1016/j.biortech.2008.11.056>
- [31] Ranz WE, Marshall WR. (1952). Evaporation from drops *Chem. Eng. Prog.* 48: 173–180. University of Wisconsin, Madison, WI.
- [32] Orang N, Tran H. (2014). Effect of feedstock moisture content on biomass boiler operation. master thesis. Chemical Engineering and Applied Chemistry University of Toronto 12.
- [33] Kaewklum R, Kuprianov VI, permchart W. (2007). Influence of fuel moisture and excess air on formation and reduction of CO and NO_x in a fluidized-bed combustor fired with Thai Rice Husk. *Asian J. Energy Environ* 8: 547- 555.
- [34] Wang Q, Zhao W, Liu H, Jia C, Xu H. (2012). Reactivity and Kinetic analysis of biomass during combustion. *Energy Procedia* 17: 869–875.
<https://doi.org/10.1016/j.egypro.2012.02.181>
- [35] Ghetti P., L. Ricca, L. Angelini, (1996). Thermal analysis of biomass and corresponding pyrolysis products. *Fuel* 75: 565-573. [https://doi.org/10.1016/0016-2361\(95\)00296-0](https://doi.org/10.1016/0016-2361(95)00296-0)
- [36] Kumar A, Wang L, Jones YA, Dzenis DD, Hanna MA. (2008). Thermogravimetric characterization of corn Stover as gasification and pyrolysis feedstock. *Biomass Bioenergy* 32: 460-467.
<https://doi.org/10.1016/j.biombioe.2007.11.004>
- [37] Khatami R, Stivers C, Joshi K, Levendis Y, Sarofim A (2012). Combustion behavior of single particles from three different coal ranks and from sugar cane bagasse in O₂/N₂ and O₂/CO₂ atmospheres. *Combust Flame* 159: 1253-1271.
<https://doi.org/10.1016/j.combustflame.2011.09.009>
- [38] Riaza J, Khatami R, Levendis YA, Álvarez L, Gil MV, Pevida C. (2014). Single particle ignition and combustion of anthracite, semi-anthracite and bituminous coals in air and simulated oxy-fuel conditions. *Combust Flame* 161: 1096-1108.
<https://doi.org/10.1016/j.combustflame.2013.10.004>
- [39] Zhou K, Lin Q, Hu H, Hu H, Song L. (2016). The ignition characteristics and combustion processes of the single coal slime particle under different hot coflow conditions in N₂/O₂ atmosphere. *Energy* 163: 173-184.
<https://doi.org/10.1016/j.energy.2016.02.038>
- [40] Ponzio A, Senthooorselvan S, Yang W, Blasiak W, Eriksson O. (2008). Ignition of single coal particles in high-temperature oxidizers with various oxygen concentrations. *Fuel* 87: 974-987.
<https://doi.org/10.1016/j.fuel.2007.06.027>
- [41] Kijo-Kleczkowska A, S´roda K, Kosowska-Golachowska M, Musiał T, Wolski K. (2016). Combustion of pelleted sewage sludge with reference to coal and biomass. *Fuel* 170: 141–160.
<https://doi.org/10.1016/j.fuel.2015.12.026>
- [42] Lu H, Ip E, Scott J, Foster P, Vickers M, Baxter LL. (2010). Effects of particle shape and size on devolatilization of biomass particle. *Fuel* 89: 1156-1168.
<https://doi.org/10.1016/j.fuel.2008.10.023>
- [43] Li J, Manosh C, Paul A, Paul L, Younger A, Ian Watson A, Mamdud Hossain B, Stephen Welch C. (2015). Characterization of biomass combustion at high temperatures based on an upgraded single particle model. *Applied Energy* 156: 749–755.
<https://doi.org/10.1016/j.apenergy.2015.04.027>
- [44] Ponzio A, Yang W, Blasiak W. (2007). Combustion of solid fuels under the conditions of high temperature and various oxygen concentrations. *International Conference on Power Engineering* 23-27.
https://doi.org/10.1007/978-3-540-76694-0_162
- [45] Williams A, Backreedy R, Habib R, Jones JM, Pourkashanian M. (2002). Modeling coal combustion: the current position, *Fuel* 81: 605-618.
[https://doi.org/10.1016/S0016-2361\(01\)00158-2](https://doi.org/10.1016/S0016-2361(01)00158-2)
- [46] Zheng G, Kozin’ski JA. (2000). Thermal events occurring during the combustion of biomass residue. *Fuel* 79: 181–192. [https://doi.org/10.1016/S0016-2361\(99\)00130-1](https://doi.org/10.1016/S0016-2361(99)00130-1)
- [47] Abuelnuor AAA, Wahid MA, Seyed Ehsan Hosseini A, Saat A, Khalid M, Saqr B, Hani H, Sait C, Osman M. (2014). Characteristics of biomass in flameless combustion: A review. *Renewable and Sustainable Energy Reviews* 33: 363–370.
<https://doi.org/10.1016/j.rser.2014.01.079>
- [48] Juan F, Pérez A, Melgar A, Benjumea PN. (2012). Effect of operating and design parameters on the gasification/combustion process of waste biomass in fixed bed downdraft reactors: An experimental study. *Fuel* 96: 487–496.
<https://doi.org/10.1016/j.fuel.2012.01.064>
- [49] Yang Y, Ryu C, Khor A, Yates N, Sharifi V, Swithenbank J. (2005). Effect of fuel properties on

- biomass combustion. Part II. Modelling approach didentification of the controlling factors. *Fuel* 84: 2116-2130. <https://doi.org/10.1016/j.fuel.2005.04.023>
- [50] Bhuiyan AA, Naser J. (2014). Effect of recycled ratio on heat transfer performance of coal combustion in a 0.5 MW th combustion test facility. 19th Aust. Fluid Mech. Conf., Melbourne.
- [51] Bhuiyan AA, Naser J. (2015). Numerical modelling of oxy fuel combustion, the effect of radiative and convective heat transfer and burnout. *Fuel* 139: 268-284.
- [52] Ryu C, Yang YB, Khor A, Yates NE, Sharifi VN, Swithenbank J. (2006). Effect of fuel properties on biomass combustion: part I. Experiments fuel type, equivalence ratio and particle size. *Fuel* 85: 1039-1046. <https://doi.org/10.1016/j.fuel.2005.09.019>
- [53] Yang YB, Yamauchi H, Nasserzadeh V, Swithenbank J. (2003). Effects of fuel devolatilisation on the combustion of wood chips and incineration of simulated municipal solid wastes in a packed bed. *Fuel* 82: 22-05. [https://doi.org/10.1016/S0016-2361\(03\)00145-5](https://doi.org/10.1016/S0016-2361(03)00145-5)
- [54] Babrauskas VJ. (2002). Ignition of wood; A review of the state of the art. *Fire Protection Eng.* 12: 163-189. <https://doi.org/10.1177/10423910260620482>
- [55] Carslaw HS, Jaeger JC. (1959). *Conduction of Heat in Solids*, second ed., Oxford Univ. Press, London, p.75.
- [56] Herman D. (1981). The rate of pyrolysis of densified ponderosa pine. Masters Thesis in Chemical Engineering at Colorado School of Mines, Golden, CO.
- [57] Olsson M. (2006). Wheat dust and peat for fuel pellets – organic compounds from combustion. *Biomass Bioenergy* 30: 555-564. <https://doi.org/10.1016/j.biombioe.2006.01.005>
- [58] Kallis KX, Giacomo A, Susini P, Oakey JE. (2013). A comparison between Miscanthus and bioethanol waste pellets and their performance in a downdraft gasifier. *Applied Energy* 101: 333-340. <https://doi.org/10.1016/j.apenergy.2012.01.037>